Journal of Thermal Science Vol.32, No.3 (2023) 1124−1154

**https://doi.org/10.1007/s11630-023-1793-z** **Article ID: 1003-2169(2023)03-1124-31**

# Discharging of PCM in Various Shapes of Thermal Energy Storage Systems: A Review

**DHAIDAN Nabeel[1*], HASHIM Hasan[1], ABBAS Abdalrazzaq[1], KHODADADI Jay[2], ALMOSAWY Wala[3], AL-MOUSAWI Fadhel[1]**

1. Engineering Faculty, Kerbala University, Kerbala, Iraq
2. Department of Mechanical Engineering, Auburn University, 1418 Wiggins Hall, Auburn, AL 36849-5341, USA
3. Al-Zahraa University for Women, Kerbala, Iraq



**Abstract:** Utilizing the phase change materials in different thermal storage applications attains valuable attention due to the fascinating thermal properties of these materials. The comprehension of the thermal behaviour of phase change materials during the melting and solidification is considered a significant priority in designing the shape of the different containers. In this review, analytical, computational and experimental investigations that address solidification/freezing of phase change materials within thermal energy storage systems are discussed. Emphasis is placed on the role of the shape of adopted containers encompassing planar, spherical, cylindrical and annular vessels. Energy storage for solar thermal applications, waste heat recovery, and thermal management of buildings/computing platforms/photovoltaics has been the topics that benefit from these investigations. For all container shapes, the freezing process is controlled initially by natural convection, and a high solidification rate is observed. Later, the conduction dominates the process, and the freezing rate declines. The temperature and flow of cooling heat transfer fluid affect the solidification process, but the impact of heat transfer fluid temperature is more significant than its flow rate. Also, the freezing time increases with the container's size and amount of contained PCM. The aspect ratio of the planar and vertical cylindrical cavities substantially influences the discharging time and rate. In contrast, the orientation of the annular cavity has a lower impact on the discharging process.

**Keywords: containers, freezing, phase change materials, phase transformation, solidification**

## 1. Introduction

### 1.1 Overview

Uninterrupted supply of dispatchable energy to residential/commercial/industrial sectors generally equipped with fossil resources/nuclear power stations has required significant technological advances in recent decades. In response to the energy crisis of the early 1970's, greater focus was placed on alternative and renewable energy sources. Since then, greater challenges with the nuclear reactors' safety and instability of pricing/supply of fossil fuel resources, in addition to more focus on the environment, have prompted greater adoption of alternative sources of energy such as solar,

Received: Jul 06, 2022
AE: GUO Shaopeng
Corresponding author: DHAIDAN Nabeel
E-mail: nabeel.sh@uokerbala.edu.iq
engnab74@yahoo.com

wave, wind, etc. It appears that the national/regional policies directed at the more comprehensive realization and utilization of such systems are widely promulgated.

### 1.2 Thermal energy storage systems

The intermittency nature of renewable energy resources requires the layout and exploitation of reliable, robust and effective thermal storage systems. The development of energy storage systems has long been considered the main obstacle to the deeper utilization of renewable energy resources. Thermal energy is characterized as the lowest grade of energy, leading to the usage of terms such as waste heat. In addition, the abundance of thermal energy such as geothermal energy, solar radiation and thermally stratified layers in oceans provides other opportunities for its conversion to proper energy forms. Based on these discussions, thermal energy storage (TES) can be considered an accumulator/ capacitor system (buffering/thermal battery). TES can provide comfortable conditions in buildings, economical energy conservation, adding to the thermal management of electronics and improving the effectiveness of industrial applications [1, 2].

### 1.3 Phase change materials and thermal conductivity enhancers

TES techniques that involve manipulation of sensible or latent energy through heating or cooling a bulk of material are identified as the thermophysical approach, whereas upon reversing the process, energy becomes available. The isothermal behaviour of phase change materials (PCM) resulted in a considerable utilization of them in TES by adopting a preference for their higher latent heat absorbed/released during phase-change conversion. The PCMs can be used effectively in many applications, such as solar systems [3], buildings [4], cooling of electronics [5], and other applications. Examples of PCM are paraffin, salt hydrates, sugar alcohols, fatty acids, etc., with their fusion temperatures varying over a wide range. In fact, various materials are appropriate for utilization in low-, medium- to high-temperature TES systems. Most PCM exhibit relatively low conductivity, which in turn leads to a degradation of transported heat during discharging/ charging processes. Including high thermal-conductivity materials (fins/wools/foams) leads to a PCM/additives component which is a logical approach. Interactions of heat transport mechanisms with the adopted configurations of these inserts remain complex issues to investigate.

Transport/thermal properties, improvement of transferred heat, encapsulation, effects of enclosure geometry and system-related issues encompassing PCM have been reported. Melting/solidification cycles of phase change are inherently time-dependent. Elucidating the relevant transported thermal mechanisms (i.e. diffusion and convection) observed in these TES and their competing/cooperating roles have not been widely discussed. Given the greater importance of TES in recent years, Fan and Khodadadi [6] reviewed literature focusing on improving the effective PCM thermal conductivity through the inserting of fins. Another review by Dhaidan and Khodadadi [7] focused exclusively on the role of high thermal conductivity fins in modifying the performance of latent heat thermal energy storage (LHTES) systems. Also, involving the metal foam, dispersing the nanoparticles, encapsulation, and multiple (cascade) PCMs can be considered as other techniques to enhance PCM performance [8–12]. Also, the influences of the operating conditions, geometrical parameters, and thermal enhancement techniques such as fins, metal foams, heat pipes, and multiple phase change materials on the melting and solidification of PCM were reviewed [13, 14]. Many articles reviewed the melting or charging of PCM in various containers [15–18]. In contrast, PCM discharging was rarely discussed in previous reviews. The present article serves as a timely discussion of the solidification of PCM in different shaped containers. The freezing of PCM in planar, spherical, cylindrical and annular vessels are reported in Sections 2, 3, 4, and 5, respectively.

### 1.4 General features of PCM discharging in any enclosure

The PCM discharging in a generic enclosure is illustrated in Fig. 1. The melting temperature, latent heat of phase-change, and thermal conductivity of PCM are denoted by $T_m$, $k$, and $\lambda$, respectively. Initially, the PCM exists in a liquid phase of temperature $T_{ini}$, where ($T_{ini}>T_m$). The thickness of the mushy zone depends primarily on the melting temperature range. Part or total of the enclosure's boundary is subjected to a cooled environment, which may be constant temperature $T_w$ ($T_w<T_m$) or connective cooling heat transfer coefficient ($h_{HTF}$) of heat transfer fluid (HTF). Consequently, the freezing front progresses from the cooled boundary toward the other parts of the enclosure. Convection dominates the early period of the freezing process. Later, as the PCM temperature decreases, the conduction develops and dominates the freezing process. The progress of the freezing front depends on the temperature difference between the PCM temperature and cooling environmental temperature ($\Delta T$). Also, the discharging process can be characterized by the Stefan number (*Ste*) and Rayleigh number (*Ra*), which are defined as:

$$Ste = \frac{C_{p\Delta T}}{L_c} \tag{1}$$

$$Ra = \frac{g\beta\Delta T L_c^3}{\alpha\upsilon} \tag{2}$$

where $C_p$, $\alpha$, $\nu$, and $\beta$ are the specific heat, thermal diffusivity, kinematic viscosity, and thermal expansion coefficient of PCM, respectively.

The characteristic length $L_c$ is identified according to the container's shape as:

$$L_c = \begin{cases} H \\ R_{in} \\ R_s - R_t \end{cases} \tag{3}$$

where $H$ is the height of the rectangular and vertical containers; $R_{in}$ represents the inner radius of the spherical and vertical cylindrical cavities, and ($R_s$–$R_t$) is the difference between the shell and tube radii of the annular enclosure.

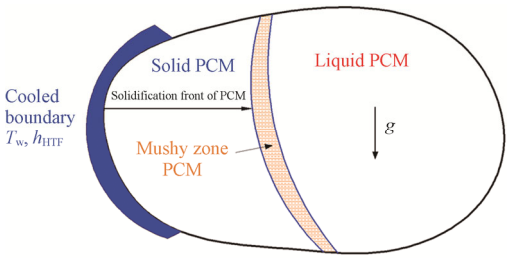


**Fig. 1** Schematic representation of the PCM discharging in the arbitrary enclosure's shape

## 2. Discharging of PCM within Planar Thermal Storage Units

Discharging and charging of PCM in planar thermal storage units is considered the most important due to its wide-range applications such as rectangular containers, plate heat exchangers, PCM panels, thermal batteries, and various PCM-integrated building construction materials (roof, walls and glazing systems), etc. Moreover, PCM's shorter melting and solidification time in these units compared to those in cylindrical cavities for the same PCM heat transfer area and volume have led attention to consider them in similar applications [19].

Jiji and Gaye [20] applied the quasi-steady approximation to analyze the melting and freezing of PCM in a 1-D slab (Fig. 2). The impact of a uniform volumetric energy generation within the slab was considered to retard the phase conversion process during solidification. The analytical results proved that complete solidification occurs without reaching a steady-state condition for a heat generation parameter above 2. In contrast, reaching a steady-state condition with incomplete solidification occurred for a heat generation parameter lower than 2.

Vynnycky and Kimura [21] performed an analytical and numerical study to examine the freezing of a PCM in a rectangular enclosure considering the natural convection. The enclosure was differentially cooled on the vertical sides, while the horizontal sides were thermally insulated (Fig. 3). The asymptotic analysis was performed regarding the Rayleigh and Stefan numbers, while the numerical simulation was solved using the finite element method. The analytical results fitted well with the computational ones for approximately 90% of the enclosure's height at all time. However, the analysis overestimated the final thickness of the solidified layer in the final 10% of the total solidification time.

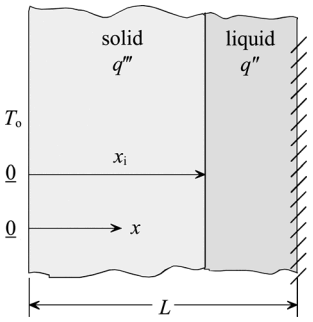


**Fig. 2** Phase-change in the 1-D slab (Jiji and Gaye [20])

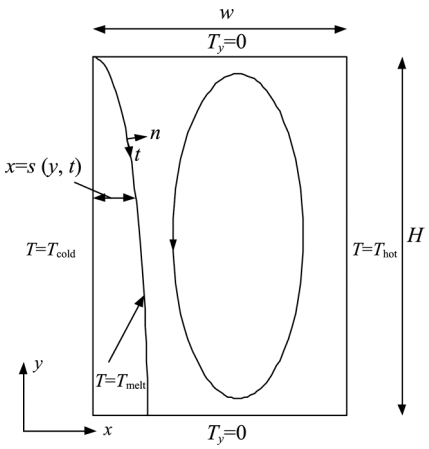


**Fig. 3** Schematic representation of the freezing in the rectangular cavity (Vynnycky and Kimura [21])

Lazaro et al. [22] tested the PCM-air heat exchanger on a real scale of two vertically-positioned prototypes. Prototype 1 used aluminium pouches filled with an inorganic PCM, while prototype 2 utilized aluminium panels filled with organic PCM. The proposed configuration was used for free cooling where the air of low temperature could be used for PCM solidification during the night, while the indoor building air could cool down through PCM melting during the next day. It was inferred that the PCM-air heat exchanger could enhance the thermal performance more than utilizing a PCM with higher thermal conductivity.

Vitorino et al. [23] investigated the kinetics of the solidification process numerically, considering the combining effects of heat conduction in the growing solidified layer, conduction through the enclosure wall and heat transfer into the cold HTF. A finite-difference method-based suitable transformation of variables has been developed for simulation. The numerical results' accuracy was achieved when compared with analytical ones, which consider only conduction through the solidified layer. Further solutions were obtained for solidification behaviour that was controlled mainly by isolating walls or by the thermal inertia of the phase change material.

Dolado et al. [24] developed an experimentally-validated one-dimensional conduction model to describe the melting/solidification of a thermal energy system consisting of a real-scale PCM-air heat exchanger (Fig. 4(a)). The PCM was macroencapsulated in aluminum slabs with bulges (Fig. 4(b)). The total quantity of organic paraffin-PCM in the thermal energy system unit was about 135 kg. The influence of the hysteresis phenomenon on thermal performance has been included in the model and considered for the PCM enthalpy-temperature curve. Also, an effective thermal conductivity was adopted to consider natural convection within the melt PCM. The solidification time was extended by 10% due to an increment in the computational value of the PCM enthalpy over its measured value. In contrast, the reduction in solidification time can be achieved by increasing the average phase change temperature and airflow rate, increasing the PCM slab's length and rugosity and decreasing the PCM slab's thickness.

Teggar and Mezaache [25] presented a conduction model to evaluate the inward solidification of a PCM (water) inside a flat plate-storage unit. Solidification was realized by circulating ethylene glycol (HTF) through parallel plates, which contained water PCM. The model was validated as its results had an agreement with the reported results in the literature. The results revealed that the solidification did not start immediately (Fig. 5) due to sensible heat resulting from the difference between initial and phase change temperatures. Also, the solidification rate decreased with time due to the additional thermal resistance of the growing solidified layer.

Iten et al. [26] experimentally explored the thermal traits of the PCM panels-air unit. The dimensions of a single PCM panel were 0.02 m×0.25 m×0.5 m. The size of the main air duct was 0.218 m×0.25 m×2.2 m. The charging and discharging time, heating/cooling load and effectiveness over the phase transition were investigated under the influence of flow rate and inlet temperature of the air. The solidification time was reduced with the increase in air flow rate. The maximum reduction in the time was observed when the air inlet velocity increased from 0.6 to 1.6 m/s. The effectiveness achieved its highest values for both melting and solidification processes for lower air inlet velocity, but the heating and cooling loads registered lower values. Moreover, it was proved that the air inlet temperature significantly impacted the solidification time.

Prieto and Gonzalez [27] studied the melting and solidification of two PCMs (RT60 paraffin and fatty acid palmitic acid) inside horizontal and vertical rectangular panels computationally. The vertical panels were subjected to isothermal conditions, while the upper and lower surfaces of the horizontal panels were kept at a fixed temperature. The influences of wall temperature and PCM thickness (aspect ratio) were analyzed. The negligible difference in the mean heat fluxes for two orientations of the plates was observed for solidification due to the vanishing role of natural convection.

Waqas and Kumar [28] evaluated the effects of inlet temperature and air flow rate on the cold accumulation in the PCM rectangular unit experimentally. The paraffin (SP29-rubitherm GmbH) was contained in the galvanized steel storage cells of dimensions 0.5 m×0.5 m×0.01 m. The PCM-air heat exchanger unit could be effectively utilized for building ventilation where the stored coolness at night was used to cool the hot ambient air during the daytime. It was observed that the time for complete solidification was reduced with a higher flow rate and

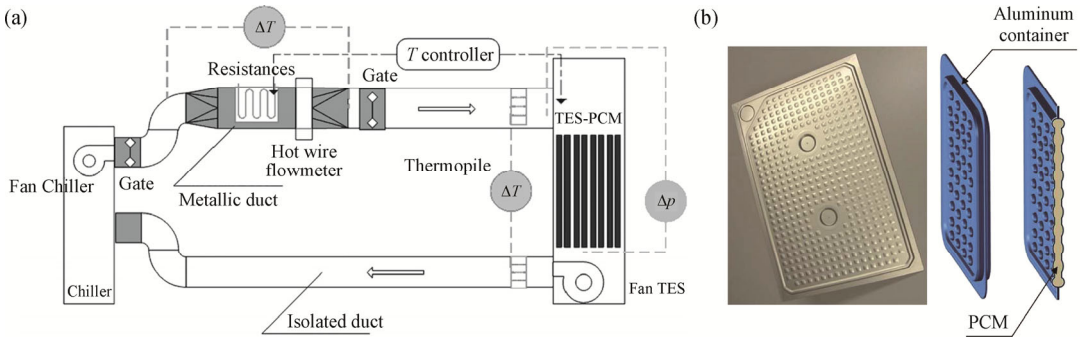


**Fig. 4** (a) Experimental setup, and (b) aluminum slabs filled with PCM (Dolado et al. [24])

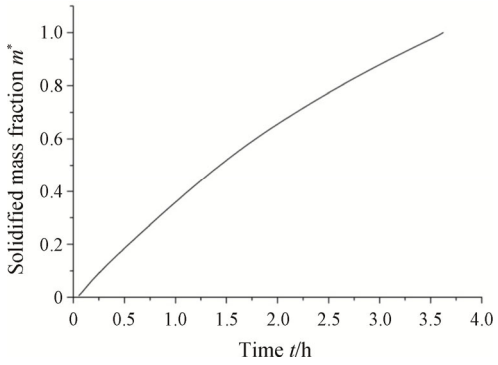


**Fig. 5** Transient solidified mass fraction (Teggar and Mezaache [25])

lower inlet temperature of the air. However, the air temperature was more pronounced in the solidification process than the airflow rate.

Hu et al. [29] verified and developed a 1-D mathematical model to describe the impact of supercooling on the PCM solidification within the plate. The predictions revealed that increasing the degree of supercooling led to an extension of the solidification process and reduced the maximum heat flux during the entire discharging process. It was deduced that neglecting the supercooling's influence caused a substantial inaccuracy in the results for PCMs to own a high degree of supercooling.

Zhou et al. [30] performed an experimental study to assert percussion vibration's effectiveness in discharging supercooled salt-PCM in a rectangular thermal storage container. Five PCM storage units were immersed in a water tank. Each unit had dimensions of 600 mm×400 mm×20 mm with a wall thickness of 1.5 mm. Percussion effectiveness was presented for assessment of percussion influence on the activation of solidification. The findings revealed that the larger momentum of percussion vibration near the cover lid and edges of the unit led to the activation of PCM solidification.

Allouhi et al. [31] presented a 2-D computational model to assess the incorporation of the PCM layer in improved water solar collector design for utilization in rural regions. Charging and discharging of n-eicosane PCM were studied for different climatic conditions, thickness and melting temperature of PCM and flow rate of HTF. The results revealed that the optimum values of PCM set temperature, PCM thickness, and mass HTF flow rate are 313 K, 0.01 m, and 0.0015 kg/s, respectively. It was observed that the melting and solidification processes were highly influenced by incident solar radiation.

Kumar et al. [32] experimentally evaluated the influences of flow rate and temperature of HTF and the energy storage capacity on the transient thermal behaviour of melting and the solidification of PCM inside a plate heat exchanger. The PCM comprised only 10% of the total mass of the system. The net PCM volume was 0.122 mL. The experimental findings revealed that the solidification process was less sensitive to the inlet temperature and flow rate of HTF.

Zarajabad and Ahmadi [33] presented a numerical investigation to determine the effective PCM volume mounted on the ceiling of a freezer cabin depicted in Fig. 6. It was pointed out that increasing the PCM thickness maintained the freezer cabin's coldness for a longer duration. The discharging time per unit of PCM mass did not vary linearly with the PCM thickness. It only increased by 3.3% as PCM thickness changed from 1 to 2 cm, but it developed by 45% when PCM thickness varied from 2 to 3 cm.

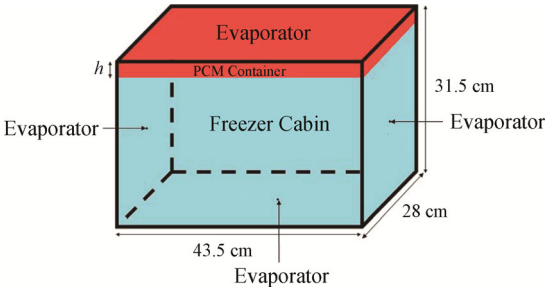


**Fig. 6** Physical model of freezer cabinet and PCM container (Zarajabad and Ahmadi [33])

Ghosh et al. [34] simulated a paraffin wax's solidification process in rectangular and spherical cavities for different sizes and thermal boundary conditions. The predictions proved that the freezing time is the lowest for the highest Stefan number and lower for the spherical cavity than for a rectangular cavity. Also, the influence of natural convection is small; solidification is considered a conduction-dominated process.

Nada et al. [35] conducted an experimental investigation to explore the charging and discharging of PCM plates and the possibility of utilizing them for building free cooling where a low-temperature difference exists between fresh air and the PCM melting temperature. The TES system involves 20 aluminium plate panels filled with the PCM. These panels were positioned horizontally in three columns in staggered distribution. Each PCM panel had dimensions of 0.42 m×0.29 m×0.015 m. The influences of flow rate, the temperature of air and the required number of PCM plates to accomplish fresh air requirements were researched. The findings indicated that the combined increase in discharge and outdoor temperature of fresh air and the number of PCM plates caused a decrease in solidification duration. Also, complete solidification of the PCM could not ensure the low-temperature difference between the PCM melting temperature and air temperature at night.

Santos et al. [36] conducted experiments on PCM charging and discharging in panels to evaluate the thermal performance of the PCM-air heat exchanger utilized as a thermal battery module. Two modules of the thermal battery were investigated: the 9-panels module (13.5 kg PCM) and the 7-panels module (17.5 kg PCM). The airflow rate was constant at 75 L/s, while the air temperature was 30°C for melting and 15°C for solidification. It was found that increasing the amount of PCM increased the amount of released/absorbed thermal energy by PCM and melting and solidification time.

Bhamare et al. [37] presented a 3-D heat transfer computational model to assess the thermal performance of charging and discharging of PCM integrated roof (Fig. 7) of different inclination angles for the climatic conditions of India in January. The predicted results showed that incorporation of the PCM in the roof structure maintained the narrow range of ceiling temperature within 25.5°C–27.5°C and reduced peak heat loads. In addition, the inclination angle of PCM-slab of 2° resulted in a 2.38°C reduction in the maximum ceiling temperature and a 16% saving in the heat gain compared with that at noon.

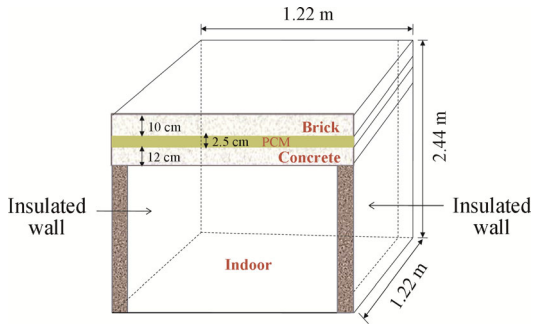


**Fig. 7** A schematic representation of the physical model (Bhamare et al. [37])

Elsheniti et al. [38] reported a dramatic reduction in computational time by proposing a novel simplified 1-D computational model (Enhanced Conduction Model, ECM) to assess the photovoltaic PV-PCM panel during melting and solidification processes. The model considered the impact of free convection by an enhanced equivalent thermal conductivity. The predicted results of the model were compared with CFD results for various aspect ratios and inclination angles. Both models were verified with the published experimental data. Insignificant deviations between the two models were observed (Fig. 8). The optimum values of inclination angles were determined for different seasons. The PV-PCM panel system showed a higher thermal performance than the PV system for all seasons. Moreover, the influence of PCM thicknesses was also evaluated.

Gürel [39] inspected the influences of different geometries of plate heat exchanger (PHE), the temperature of HTF and the kind of PCM and its thickness on the solidification of PCM. The PCM involved in the space between corrugated steel plates of PHE, as shown in Fig. 9. It was concluded that the solidification time was reduced by decreasing the phase change temperature and thickness of PCM and lowering the inlet temperature of HTF. Also, for the same geometric features, operating conditions and PCM volume, it was found that the freezing time of the PHE storage system was decreased by 63% compared to that exhibited by the cylindrical storage unit.

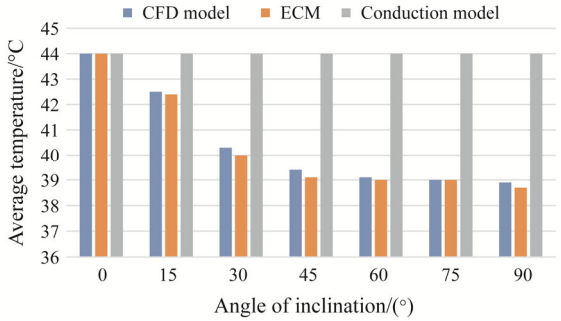


**Fig. 8** The average temperature of the front surface at different inclination angles (Elsheniti et al. [38])

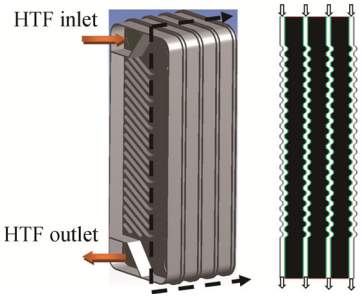


**Fig. 9** Schematic representation of a corrugated PHE-PCM system (Gürel [39])

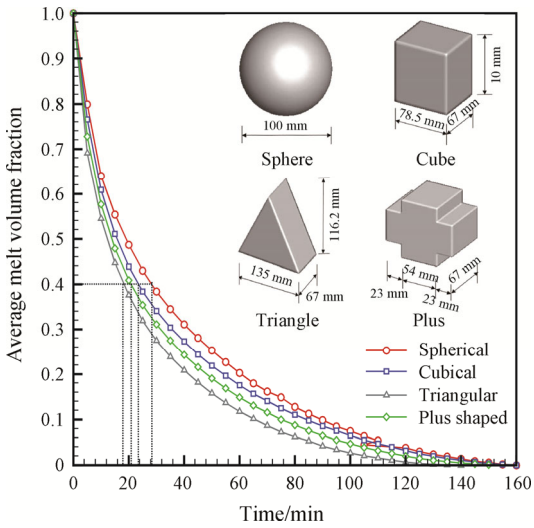


**Fig. 10** Liquid fraction for various capsule shapes (Patel et al. [40])

**Table 1** Summary of investigations on PCM freezing inside planar TES units

| Authors (Year) | Configuration Conditions | PCM ($T_m$, $\lambda$) | Type of Study | Highlighted Results/Findings |
|---|---|---|---|---|
| Jiji and Gaye [20] (2007) | Solidification in a 1-D slab | Nuclear material $UAI_x$ (660°C, 39.9 W/(m·K)) | Analytical (quasi-steady approximation) | The amount of heat generation controlled the steady-state reaching and solidification completion. |
| Vynnycky and Kimura [21] (2009) | Freezing in a rectangular enclosure cooled differentially on the vertical surfaces | Water (0°C, 0.578–1.918 W/(m·K)); gallium (29.78°C, 32 W/(m·K)); and lauric acid (43.5°C, 0.6098 W/(m·K)) | Analytical (asymptotic analysis) and Numerical (FEM) | Good agreement was achieved between the analytical and computational solutions for approximately 90% of the enclosure's height at all times. |
| Lazaro et al. [22] (2009) | Discharging and charging of PCM in two prototype configurations | Commercial inorganic PCM (NA, 0.7 W/(m·K)), and commercial organic (NA, 0.16 W/(m·K)) | Experimental (real-scale) | The PCM-air heat exchanger could enhance thermal performance more than utilizing a PCM with higher thermal conductivity. |
| Vitorino et al. [23] (2010) | Solidification in a planar reservoir cooled by HTF | Several kinds of PCM | Numerical (conduction through solid PCM, immobilization of moving boundaries, FDM ) | Good agreement was achieved between the numerical results and the analytical results that consider only conduction through the solidified layer. |
| Dolado et al. [24] (2011) | PCM in aluminium rigid slabs charged and discharged by air | Commercially organic paraffin (27°C, $\lambda$ function of temperature) | Experimental and Numerical (1-D conduction analysis, FDM) | Variation of the solidification time can be performed by altering the operating conditions, such as the average phase change temperature and the airflow rate and geometry conditions, such as length, rugosity and the thickness of the PCM slab. |
| Teggar and Mezaache [25] (2013) | Solidification of water contained between two cold plates | Water (0°C, 0.23–0.6 W/(m·K)) | Numerical (1-D conduction analysis, CVA) | The solidification rate decreased with time due to the additional thermal resistance of the growing solidified layer. |
| Iten et al. [26] (2016) | Solidification and melting of PCM panel-air heat exchanger unit | RT25 (23–25°C, 0.2 W/(m·K)) | Experimental | The solidification time was reduced with the increase in airflow rate.<br>The air inlet temperature had the most significant impact on the solidification time. |
| Prieto and Gonzalez [27] (2016) | Solidification and melting of PCM inside horizontal and vertical panels | RT60 paraffin (53–61°C, 0.2 W/(m·K)), fatty acid (65°C, 0.16–0.32 W/(m·K)), and palmitic acid (64.5°C, NA) | Numerical (EPM, FVM) | The solidification of PCM showed a negligible difference in the mean heat fluxes for two orientations of the plates. |
| Waqas and Kumar [28] (2016) | Air-PCM panels storage unit for building ventilation | SP29 (28–29°C, 0.6 W/(m·K)) | Experimental | The solidification time decreased at a higher flow rate and lower inlet temperature of the air.<br>The influence of air temperature was more pronounced on the solidification process than the airflow rate. |
| Hu et al. [29] (2017) | Solidification of PCM in a 1-D plate with the effect of supercooling | PCM (26–28°C, 0.2 W/(m·K)) | Numerical (1-D conduction analysis, equivalent specific heat capacity method, FDM) | Supercooling caused a delay in the solidification process and a reduction in the maximum heat flux during the entire discharging process. |
| Zhou et al. [30] (2017) | Solidification of PCM in a rectangular container under the effect of percussion vibration | Sodium acetate salt solution (58°C, NA) | Experimental | Percussion vibration can be used as a trigger tool for the solidification of supercooled PCM in the seasonal solar heating system. |
| Allouhi et al. [31] (2018) | Melting and solidification of PCM-incorporated water solar collector | N-eicosane (36.65°C, 0.16–0.212 W/(m·K)) | Numerical (EPM, FVM) | The values of PCM thickness, PCM set temperature and mass flow rate of HTF that achieved the optimum performance were specified.<br>The melting and solidification processes were highly influenced by incident solar radiation. |

**(Continued Table 1)**

| Authors (Year) | Configuration Conditions | PCM ($T_m$, $\lambda$) | Type of Study | Highlighted Results/Findings |
|---|---|---|---|---|
| Kumar et al. [32] (2018) | Melting and solidification of PCM inside the plate heat exchanger | PureTemp 29 (29°C, 0.15–0.25 W/(m·K)) | Experimental | The flow rate and inlet temperature of HTF have a small effect on the solidification process. |
| Zarajabad and Ahmadi [33] (2018) | PCM container mounted on the ceiling of freezer cabinet | eutectic solution NaCl-$H_2O$ (–21°C, 0.57 W/(m·K)) | Numerical (EPM, FVM) | The discharging time per unit of PCM mass did not enhance linearly with the PCM volume. |
| Ghosh et al. [34] (2019) | Solidification in spherical and rectangular cavities | RT27 (28–30°C, 0.15 W/(m·K)) | Numerical (VOF, EPM, FVM) | The solidification decreased with the Stefan number, which is lower for a spherical cavity than a rectangular cavity. |
| Nada et al. [35] (2019) | Charging and discharging of PCM in plates | SP 24E (NA, NA) | Experimental | Increasing the outdoor temperature and discharge of fresh air and the number of PCM plates decreased the freezing time.<br>Low-temperature difference between PCM and fresh air could not ensure complete solidification of PCM. |
| Santos et al. [36] (2019) | Two different modules of thermal batteries (PCM panels-air heat exchanger) | Industry recognized PCM (21–24°C, NA) | Experimental | The melting and solidification time increase with the amount of contained PCM. |
| Bhamare et al. [37] (2020) | Melting and solidification of PCM-integrated roof | Inorganic salt hydrate (26–28°C, 0.54–1.09 W/(m·K)) | Numerical (EPM, FVM) | Incorporating PCM slab into roof structure maintained uniform roof temperature and reduced heat load.<br>The suitable inclination of the PCM slab attained the best performance and improved melting and solidification cycles. |
| Elsheniti et al. [38] (2020) | Solidification in PV-PCM panel | RT25HC (25–27°C, 0.18–0.19 W/(m·K)) | Numerical (1-D enhanced conduction model & CFD model-based FVM) | Dramatic saving in computational time was observed due to utilizing the 1-D enhanced conduction model compared with the CFD model. Optimum seasonal inclination angles were specified. |
| Gürel [39] (2020) | Corrugated plate heat exchanger | RT-35 (28–40°C, 0.1–0.2 W/(m·K)) and n-octadecane (28.2°C, 0.1505 W/(m·K)) | Numerical (EPM, FVM) | The effects of HTF temperature, thickness and type of PCM and geometric layout of the PHE were investigated.<br>The solidification time of the PHE-PCM unit was reduced by 63% compared to that of the cylindrical-PCM unit for the same conditions and the same volume of PCM. |
| Patel et al. [40] (2020) | Charging and discharging of PCM inside different shapes of macro-capsules | Paraffin wax (58–60°C, 0.25 W/(m·K)) | Numerical (EPM, FVM) | The triangular capsule had a higher thermal performance during melting and solidification processes, among other capsules. |

CVA: control volume approach; EPM: enthalpy-porosity method; FDM: finite difference method; FEM: finite element method; $k$: thermal conductivity; $T_m$: melting temperature; FVM: finite volume method; VOF: the volume of the fluid model.

Patel et al. [40] conducted a comprehensive computational study to inspect PCM's charging and discharging behaviour inside various shape macro-capsules. The considered capsules were cubical, spherical, triangular, and plus. The experimental facility was developed to validate the computational model. The conduction mechanism dominates the solidification process; however, natural convection prevailed in the process's initial duration. Also, it was found that the triangular capsule attained a higher thermal performance during melting and solidification processes, among other capsules. The PCM freezing duration in the triangular capsule was shortened by 15.82% lower than that of the spherical capsule (Fig. 10). Moreover, the reduction of 27% in the triangular capsule size led to a decrease of 19.17% in solidification time.

A summary of the studies associated with the solidification of PCM within planar TES units is provided in Table 1. It is released from the above literature that the solidification time varies inversely with the melting temperature range of the PCM and the thickness of the planar cavity. Also, the solidification time decreased with the increase of flow rate or/and the decrease in inlet temperature of the HTF. In addition, the initial temperature of PCM has an insignificant effect on the freezing duration, but the surface temperature dramatically influences the solidification process.

## 3. Freezing of PCM in Spherical TES Capsules

Among the various geometrical configurations of containers holding PCM, spherical shells exhibited the best thermal performance due to their high value of the outer surface area relative to the quantity of PCM material that can be encapsulated [41]. In addition, the shortest time for thawing and freezing were related to the spherical capsules [42]. Moreover, a spherical capsule is easily fabricated and packed in thermal energy storage devices.

Chan and Tan [43] carried out experiments on the discharging of PCM inside an aluminium spherical capsule under various surface temperatures (3°C, 8°C, and 13°C) and different initial liquid superheats (0°C, 2°C, and 8°C). It was observed that the freezing rate was large, and the freezing front propagated concentrically toward the center of the sphere during the initial periods of the solidification process. As time travelled, the freezing rate deteriorated, and the freezing front was irregular due to the shrinkage of the solid PCM and voids formation. Moreover, the PCM initial liquid-superheat showed an insignificant effect (Fig. 11(a)) on the solidified PCM, while the surface temperature indicated an important influence (Fig. 11(b)).

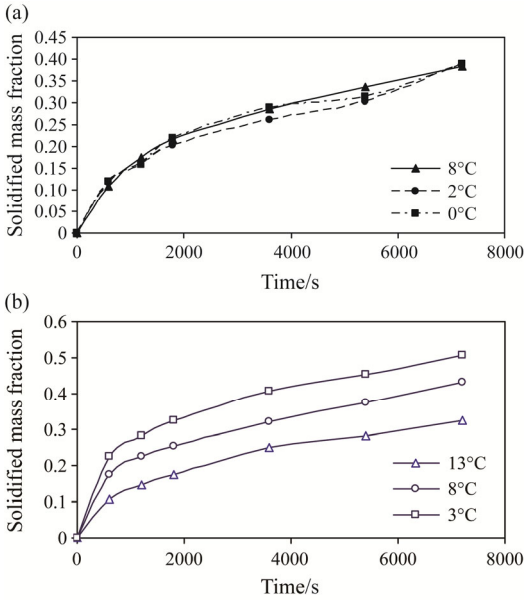


**Fig. 11** Solid fraction variation with (a) various initial liquid superheat, and with (b) different surface temperatures (Chan and Tan [43])

Ismail and Moraes [44] explored the solidification of various PCM (water and mixtures of water with different Glycol contents) in a spherical vessel. The influences of surface temperature (–25°C to –5°C), diameter (0.035–0.131 m) and the material of the vessel (plastic and glass) were considered. It was indicated that the freezing time increased with the Glycol content and surface temperature, and diameter of the vessel. Also, increasing the thermal conductivity of the vessel's material led to an acceleration of the solidification process.

Veerappan et al. [45] developed validated analytical models to evaluate the charging and discharging of five PCM types within the spherical capsules. The models considered conduction, natural convection, and heat generation. The predictions pointed out that the $CaCl_2 \cdot 6H_2O$ PCM achieved excellent freezing and thawing features; therefore, it can be used effectively for solar latent heat storage applications. Also, the initial temperature of PCM had an insignificant influence on the solidified fraction.

Wu et al. [46] introduced a computational study to examine the thermal features of thawing and freezing of n-tetradecane PCM inside spherical capsules of packed bed cool thermal energy storage systems. A higher cool stored and released rate was observed at the initial time, and afterwards, they decayed as time progressed. Increasing the HTF inlet temperature and/or decreasing the flow rate of HTF caused an extension of time for complete discharging. Also, the solidification time was increased for the lower porosity of the packed bed. Next,

Wu and Fang [47] simulated the freezing of myristic acid PCM. Water was used as HTF in the thermal storage system with a solar heating collector (Fig. 12). It was found that the latent efficiency (the instantaneous released latent heat divided by the maximum released heat) was increased with the inlet temperature of HTF. Also, no significant impact of the initial temperature of the packed bed on the solidification time was found.

ElGhnam et al. [48] evaluated the influence of design parameters of the storage unit (size and material) and operating conditions of HTF (temperature and flow rate) on the discharging and charging of water within the spherical cavity experimentally. The spherical vessels were fabricated from various materials (stainless steel, copper, brass, plastic, and glass) with different diameters (0.042–0.11 m) of thickness 0.001 m. The experimental outcomes exhibited that the discharging rate was accelerated by employing metallic and small size capsules, and lower temperature and higher flow rate of HTF. Also, it was found the thermal conductivity of the vessel material had a relatively insignificant influence on the solidification characteristics.

Archibold et al. [49] numerically analyzed the influences of the Grashof, Stefan and Prandtl numbers on discharging sodium nitrate in a spherical capsule. The PCM filled the capsule partially, while the air was contained in the top part of the capsule. A finite volume-based enthalpy-porosity technique and volume-of-fluid model were utilized to simulate the freezing front and PCM-air interface. The results indicated that decreasing the temperature variation between the melting temperature and capsule's surface temperature from 5°C to 15°C resulted in a 25% decrease in freezing duration. Also, the role of natural convection had a smaller contribution to the thermal behaviour of the freezing process than conduction.

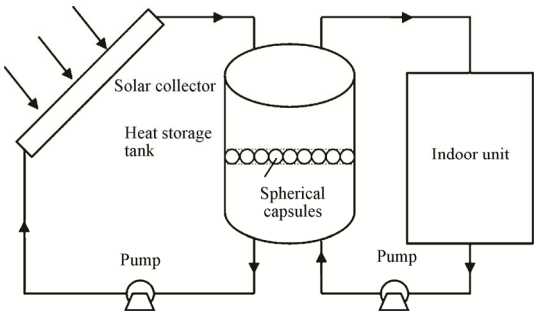


**Fig. 12** Schematic configuration of solar thermal packed bed storage system (Wu and Fang [47])

Elmozughi et al. [50] presented a 3-D numerical model to examine the melting and solidification process of high-temperature PCM (sodium nitrate) in the spherical capsule of a 20% air void. The capsule was 22 mm in diameter and at a constant-wall temperature. It was observed that the solidified molten salt began at the bottom of the capsule and progressed upward gradually, as observed in Fig. 13. The growing solidified PCM suppressed the exchanged heat between the liquid PCM and cold HTF, which extended the solidification time. In addition, the discharging time was ten times longer than the charging time.

Reddy et al. [51] investigated the impact of the material of the capsule's wall on the melting and solidification of PCM inside spherical capsules experimentally. The diameter of the capsule was 68 mm. The capsules employed materials: aluminium, high-density polyethylene (HDPE), and mild steel. The storage unit was integrated with a flat plate solar collector where water was utilized as HTF. An insignificant effect of the capsule's material on the thermal feature of the TES unit was indicated.

Chandrasekaran et al. [52] experimentally explored the freezing features of water (PCM) in a spherical storage cell with different fill volumes (80%, 85%, 90%, 92% and 95%) for various surrounding bath temperature conditions (–12°C, –9°C, –6°C, and –3°C). The cell was made of low density polyethylene with a diameter of 69 mm. It was inferred that increasing the PCM fill volume alleviated the supercooling problem, which was eliminated at a fill volume of 95%. Also, earlier onset of the discharging and reduction in the solidification

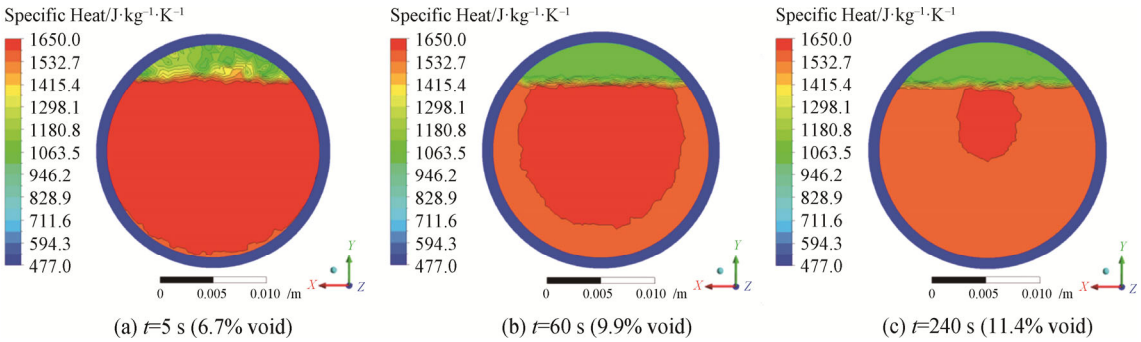


(a) $t$=5 s (6.7% void) (b) $t$=60 s (9.9% void) (c) $t$=240 s (11.4% void)

**Fig. 13** The solid-liquid interface during solidification at various time instants (Elmozughi et al. [50])

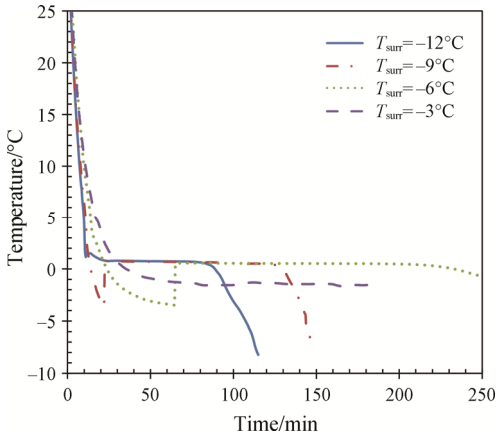


**Fig. 14** Impact of the bath temperature on the temperature at the center of the capsule for the case of 90% fill volume (Chandrasekaran et al. [52])

time was observed when increasing the fill volume. On the other hand, the HTF temperature influenced the commencement of freezing, as illustrated in Fig. 14. The same authors [53] performed experiments to inspect the discharging traits of water-PCM-filled 90% of stainless spherical vessels of various diameters (74–100 mm). The vessels were subjected to different surrounding bath temperatures (–12°C, –9°C, and –6°C). The experimental outcomes indicated that the subcooling effect was decreased with the increase in the vessel diameter and was eliminated totally at higher temperature potential for all the vessel diameters. Also, the freezing interface rapidly progressed in the larger vessel than the smaller one until 75% of the water mass was solidified, and this influence was clearer at higher temperature driving potential.

Asker et al. [54] applied the control volume approach and temperature transforming method to examine the inward solidification inside a spherical capsule numerically. The storage unit was subjected to a convective heat transfer environment of coolant fluid. The predictions indicated that the freezing time was shortened with the decrease of the diameter of the capsule and the coolant fluid temperature. Meanwhile, the entropy generation varied positively with the capsule size and fluid temperature.

Ismail et al. [55] performed experiments to assess the influences of the wall temperature (–20°C to –5°C) and size of the spherical shell (35–131 mm in diameter), and the initial temperature of PCM at the time of charging and discharging processes. In addition, the results of these time durations were correlated with the influencing factors. The findings revealed that decreasing the wall temperature or reducing the concentration of polyethylene glycol resulted in shortening the solidification time. Also, there was a good agreement between predicted results from correlations and experimental measurements, with maximum differences being lower than 10%.

Liu et al. [56] proposed an experimental technique to examine the inward discharging of PCM contained in stainless steel spherical capsules of diameter 59.6 mm quantitatively. The method depended on the PCM's dynamic measurement of transient volume shrinkage. The monitoring of the descending liquid PCM in the scaled tube is illustrated in Fig. 15. The agreement between the measured volume shrinkage and the maximum theoretical values at the end of the discharging process indicated the reliability and verification of the proposed technique. Measured values of the solidification fraction and surface-averaged Nusselt number were correlated with the Fourier and Stefan numbers.

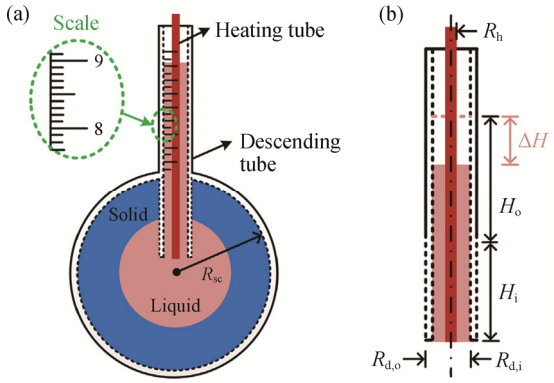


**Fig. 15** Schematic diagrams of the test section and the scaled tube of liquid PCM (Liu et al. [56])

Pop et al. [57] developed a simple mathematical model to describe the thermal behaviour of the melting/solidification PCM inside a spherical shell. They reported that the validated mathematical model could be utilized effectively to analyze thermal-flow behaviour in the latent TES unit.

Ehms et al. [58] computationally examined the solidification process of the erythritol-PCM in a spherical vessel that was cooled by HTF. The influences of the capsule's diameter and wall temperature were examined as presented in Fig. 16. It was found that at the beginning of the solidification process, the rate of formation of the solid phase was high. Later, the heat flux was reduced due to the growth of the solid layer and the associated thermal resistance. Also, it was confirmed that the vessel's size was the main impact on the discharging process. Furthermore, the liquid fraction was correlated as a function of the Fourier and Stefan numbers, thus adjusting the existing correlations in previous works.

Nazififard et al. [59] developed a computational model that was validated experimentally to simulate paraffin wax-PCM's solidification inside a spherical cavity with constant wall temperature. For the same initial and wall temperatures, it was found that utilizing a smaller cavity

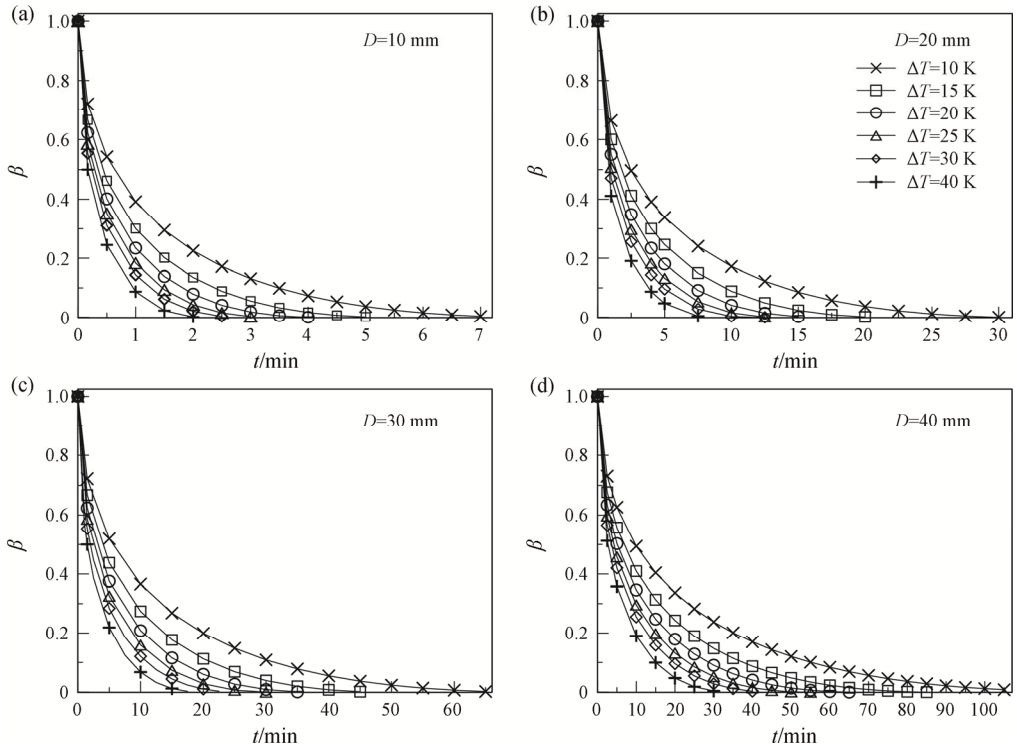


**Fig. 16** Instantaneous liquid fraction for different sizes of sphere and wall temperature (Ehms et al. [58])

led to an acceleration in the solidification of PCM. Also, the wax near the cavity's inner wall solidified quicker than at the cavity center.

Loem et al. [60] experimentally and numerically studied the melting and freezing of RT-42 PCM inside celluloid balls of a 0.04 m diameter which were heated and cooled by air. The time required for solidification increased with the PCM thickness. On the other hand, the solidification period was shortened by increasing the mass flow rate of air for all PCM thicknesses. Also, the results of estimated instantaneous air temperature leaving the bed for various PCM bed thicknesses and airflow rates were correlated for both charging and discharging processes.

Mawire et al. [61] experimentally inspected the melting/solidification of PCM encapsulated in a spherical aluminium cell of 0.05 m in diameter. Four PCM were considered: erythritol, adipic acid, high-density polyethylene (HDPE) and eutectic solder. The sunflower oil with different flow rates (4, 6, and 8 mL/s) was utilized as HTF to charge/discharge the PCM. The experimental findings revealed that the eutectic solder experienced the most effective thermal characteristics during both thawing and freezing cycles. The discharging time was reduced with the increase in the HTF flow rate. Also, adding nucleating agents enhanced erythritol and adipic acid's phase change transition characteristics.

Vikram et al. [62] fulfilled experiments to inspect the solidification characteristics of deionized water dispersed with additives of soluble salts and nucleating agents at

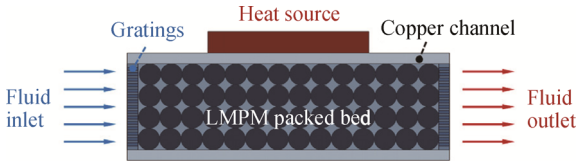


**Fig. 17** Schematic representation of composite heat sink (Gao et al. [63])

various concentrations in a spherical encapsulation. The additives of sodium chloride and D-sorbitol were utilized to reduce or eliminate the major problem of subcooling in water. It was observed that adding 0.5 wt% sodium chloride exhibited lower subcooling. In addition, increasing the sodium chloride dispersion led to increased viscosity, decreased thermal conductivity, and delay in the formation of nucleation sites. Also, dispersion of D-sorbitol resulted in a faster rate of nucleation sites' creation.

Gao et al. [63] developed a 3D numerical model that was validated experimentally to inspect the thermal characteristics of the composite heat sink. The sink was packed with the low melting point metal (LMPM) spherical macrocapsules filled with PCM (Fig. 17). The system exhibited an excellent thermal management performance compared to a heat sink cooled by convection. It was concluded that increasing the flow rate of the HTF and/or reducing the size of spherical LMPM-PCM macrocapsules resulted in decreasing the heat source average temperature and shortening the period of the de-pulse stage and duration of the solidification.

**Table 2** Outline of studies on PCM solidification within spherical capsules

| Authors (Year) | Configuration and Conditions | PCM ($T_m$, $\lambda$) | Type of Study | Highlighted Results/Findings |
|---|---|---|---|---|
| Chan and Tan [43] (2006) | Discharging in a capsule for various surface temperatures and initial liquid-superheat | N-hexadecane (18.2°C, NA) | Experimental | The freezing rate was large during the initial periods of the solidification process. As time travelled, the freezing rate deteriorated.<br>The PCM initial liquid superheating showed an insignificant effect on the solidified PCM, while the surface temperature indicated an important influence. |
| Ismail and Moraes [44] (2009) | Freezing in a vessel of different materials, surface temperatures, and diameters | Water and different contents of water-Glycol solutions (various $T_m$ and $\lambda$) | Experimental and Analytical (pure conduction model) | The freezing time increased with the increase of Glycol content, surface temperature, and vessel diameter.<br>Increasing the thermal conductivity of the vessel's material led to an acceleration of the solidification process. |
| Veerappan et al. [45] (2009) | Solidification and melting of different PCMs under the effect of surface temperature, PCM initial temperature and capsule diameters | Capric/lauric acid (18°C, 0.139–0.143 W/(m·K)), $CaCl_2 \cdot 6H_2O$ (29°C, 0.53–1.09 W/(m·K)), n-Octadecane (27.5°C, 0.157–0.39 W/(m·K)), n-Hexadecane (18°C, 0.1562–0.43 W/(m·K)), and n-Eicosane (36.4°C, 0.146–0.462 W/(m·K)) | An analytical model considering conduction, convection, and heat generation | The $CaCl_2 \cdot 6H_2O$ PCM achieved excellent freezing and thawing features than other PCMs.<br>The initial temperature of PCM had an insignificant influence on the solidified fraction. |
| Wu et al. [46] (2010) | Solidification/melting in a cavity surrounded by aqueous ethylene glycol as HTF | N-tetradecane (2.73–7.79°C, 0.211–0.273 W/(m·K)) | Numerical (Energy balance, FDM) | Solidification time was increased by increasing the HTF inlet temperature, decreasing the flow rate of HTF, and employing a packed bed with lower porosity. |
| Wu and Fang [47] (2011) | Solidification in a vessel surrounded by water as HTF | Myristic acid (58°C, 0.15 W/(m·K)) | Numerical (Energy balance, FDM) | Latent efficiency was increased with the inlet temperature of HTF.<br>The influence of the initial temperature of the packed bed was insignificant on the solidification time. |
| ElGhnam et al. [48] (2012) | Charging and discharging in cavity placed in a tank of aqueous ethylene glycol solution | Water (0°C, NA) | Experimental | The freezing time was decreased by utilizing a small-size metallic cavity, increasing the flow rate of HTF and reducing the temperature of HTF. |
| Archibold et al. [49] (2014) | Solidification in capsule cooled isothermally | Erythritol (306.3–306.8°C, temperature-dependent) | Numerical (VOF, EPM, FVM) | Reducing the wall temperature decreases the solidification time.<br>Conduction dominated the solidification process. |
| Elmozughi et al. [50] (2014) | Solidification/melting due to constant wall temperature | Sodium nitrate (308°C, 0.5 W/(m·K)) | Numerical (VOF, EPM, FVM) | The discharging time was 10 times longer than the charging time. |
| Reddy et al. [51] (2014) | Thawing and freezing in storage unit integrated with flat plate solar collector | Paraffin wax type II (61°C, 0.15–0.4 W/(m·K)) | Experimental | Insignificant effect of capsule material on the thermal behaviour of storage cell |
| Chandrasekaran et al. [52] (2015) | Solidification in capsule immersed in a constant temperature bath | Water (0°C, NA) | Experimental | Increasing the volume fill ratio of PCM reduced the effect of subcooling and shortened the solidification time. |
| Chandrasekaran et al. [53] (2015) | Solidification in capsule surrounded by HTF | Water (0°C, NA) | Experimental | For all the capsule sizes, the subcooling effect was reduced with the capsule size increment.<br>The optimal thermal energy storage design can be achieved by employing a larger vessel size with adequate temperature potential. |

**(Continued Table 2)**

| Authors (Year) | Configuration and Conditions | PCM ($T_m$, $\lambda$) | Type of Study | Highlighted Results/Findings |
|---|---|---|---|---|
| Asker et al. [54] (2016) | Solidification in capsule subjected to a convective cooling environment | Water (0°C, 0.567–1.88 W/(m·K)) | Numerical (CVA-based temperature transforming method) | The coolant fluid temperature and the size of the capsule play a significant role in the layout and evaluation of the thermal performance and entropy generation of energy storage systems. |
| Ismail et al. [55] (2016) | Solidification/melting in vessel immersed in HTF bath | Water (0°C, NA) and mixtures of water and polyethylene glycol (NA, NA) | Experimental | Good agreement was indicated between correlated results and experimental measurements with maximum differences lower than 10%. |
| Liu et al. [56] (2016) | Inward solidification in capsule immersed in the cooling tank | 1-tetradecanol (37°C, 0.159–0.252 W/(m·K)) | Experimental | The solidification fraction was measured by the shrunk volume of PCM.<br>The measured data of the Nusselt number and solid fraction were correlated with the Fourier and Stefan numbers. |
| Pop et al. [57] (2017) | Spherical vessel charged and discharged by air | RT-20 (21.5°C, NA) | Numerical (Energy balance) | The validated model could be utilized effectively to evaluate the thermal features of the PCM storage system. |
| Ehms et al. [58] (2018) | Solidification due to flowing HTF around the capsule | Erythritol (118°C, 0.326–0.733 W/(m·K)) | Numerical (EPM, FVM) | Initially, the solidification rate is high and decreases with the growth of the solid layer.<br>The capsule's diameter influenced more than the wall temperature. |
| Nazififard et al. [59] (2018) | Solidification in vessel maintained at a constant temperature | Paraffin wax (56–58°C, 0.167–0.212 W/(m·K)) | Experimental and Numerical (EPM, FVM) | The solidification time was decreased with decreasing the size of the cavity. |
| Loem et al. [60] (2019) | Spherical balls were charged and discharged by air | RT-42 (38–43°C, 0.2 W/(m·K)) | Experimental and Numerical (Energy balance-based CVA) | The solidification period varied positively with the bed PCM thickness and inversely with the airflow rate. |
| Mawire et al. [61] (2019) | Aluminium capsule in a bath of flowing sunflower oil (melting and solidification) | Erythritol (118–122°C, 0.13 W/(m·K)), adipic acid (150–152°C, 0.142–0.162 W/(m·K)), HDPE (130°C, 0.38–0.51 W/(m·K)) and eutectic solder (183°C, 50 W/(m·K)) | Experimental | The eutectic solder experienced the best thermal characteristics during both thawing and freezing cycles.<br>Increasing the HTF discharge caused a shortening in discharging time. |
| Vikram et al. [62] (2019) | Solidification of PCM dispersed with nucleation agents in capsule cooled by HTF | Deionized water (0°C, NA) | Experimental | The increase of dispersants in the subcooling region caused a decrease in the cooling rate. |
| Gao et al. [63] (2020) | Heat sink composed of LMPM-PCM spherical macrocapsules cooled by flowing HTF | 20 mL E-BilnSn with 40 mL Ecoflex 00–30 (NA, NA) | Numerical (Equivalent heat capacity method) | The system exhibited an excellent thermal management performance compared with a convective cooling heat sink.<br>Rising the HTF discharge and/or reducing the size of spherical LMPM-PCM macrocapsules resulted in shortening the freezing time. |
| Lago et al. [64] (2020) | Freezing and fusion in shell mounted in constant temperature tank | Water (0°C, 0.56–2.25 W/(m·K)) or a mixture of polyethylene glycol and water (4–8°C, 0.06 W/(m·K)) | Experimental | Increasing the capsule size and capsule temperature led to an increase in the solidification time.<br>An agreement was attained between correlated and experimental results of the freezing time. |
| Gao et al. [65] (2020) | Solidification and melting in capsules due to flowing HTF (water) | Paraffin C17 (NA, 0.21 W/(m·K)) | Numerical (EPM, FVM) | Increasing the thickness of the solidified layer of PCM resulted in a decrease in transmitted heat by convection between liquid PCM and the storage unit wall. |
| Lipnicki et al. [66] (2022) | Solidification in cavity cooled on its surface | RT64HC (64.2°C, NA), water (0°C, NA) | Analytical (pure conduction model) and Experimental | The theoretical model could be effectively used for evaluating the freezing process. |

Lago et al. [64] inspected the influences of the size and the temperature of the spherical shell (35–131 mm) and the initial temperature of PCM on the charging and discharging time experimentally. Water or a mixture of polyethylene glycol and water were tested as PCM. It was deduced that increasing the polyethylene glycol content in the PCM resulted in an extension of the duration of solidification for all wall temperatures of the shell. Also, the freezing time was increased with the rise in the diameter of the spherical shell and wall (or bath) temperatures. The resulting correlation for the freezing time agreed well with experimental data with 5.91% as a maximum discrepancy.

Gao et al. [65] performed a computational study to analyze the thawing and freezing processes of PCM in a spherical cell interconnected with heat pump system. It was observed that an increase in the thickness of the solidified layer of PCM during the solidification process led to a reduction in convection between liquid PCM and the wall of the spherical wall. Besides, the solidification process was affected significantly by the diameter of the spherical vessel.

Lipnicki et al. [66] developed a simple analytical model depending on a conjugate differential equation system to assess the solidification of PCM inside a spherical cell. Also, the experiments were conducted to validate the theoretical model. The experimental findings of the freezing front were consistent with the predicted ones from the model, in which the natural convection of liquid melt was not considered.

An outline of the studies dedicated to the freezing of PCM within spherical capsules is presented in Table 2. It is inferred from the discussion of the above literature that the diameter or the size of the spherical capsules and the cooling environmental temperature has a major impact on the discharging time of the PCM. Also, the influence of the initial superheat is negligible.

## 4. Solidification of PCM in Cylindrical Thermal Storage Vessels

Cylindrical vessels that contain PCM can be utilized as plain tube heat exchangers where PCM can exchange thermal energy with external circulating HTF. These vessels have simple geometry and can be fabricated using straightforward manufacturing methods. Along with spherical capsules, cylindrical vessels are preferred for thermal energy storage applications due to their favourable surface area-to-volume ratio [67].

Bilir and Ilken [68] applied the control volume approach to explore numerically the inward freezing of PCM encapsulated in cylindrical or spherical containers. The total freezing time was correlated with the Biot number, the Stefan number, and superheat parameter. The resulting correlations were reliable and could be used in many engineering applications with high accuracy.

Kalaiselvam et al. [69] proposed validated analytical models to examine the melting and solidification of three PCM types inside cylindrical containers. The "conduction" model and "conduction and heat generation" model were used to analyze the solidification process. It was found that the model considering the conduction and heat generation was more accurate in predicting the freezing front. The predictions proved that the freezing time varies positively with the Stefan number and inversely with the heat generation parameter. Furthermore, the 60% n-tetradecane + 40% n-hexadecane mixture PCM indicated more excellent phase-change characteristics than the two other kinds of PCM.

Lu et al. [70] presented a numerical investigation to analyze the solidification and melting phenomena during the cold filling process of molten salt inside a horizontal cylindrical pipe using the volume-of-fluid model. The predicted results showed the maximum thickness of solidified layer caused a maximum flow velocity. Also, the boundary heat flux decreased in the thawing process and increased in the freezing process. Furthermore, it was found that the inlet conditions of flow (inlet temperature and inlet velocity) could significantly affect the filling characteristics.

Rajeev and Das [71] presented a numerical solution of inward discharging of liquid PCM in cylindrical and spherical containers cooled isothermally. For both containers, the solid-liquid interface's velocity decreased with the Stefan number, and it was reduced as the interface moved towards the center of the containers. In addition, for the same Stefan number, the freezing duration of PCM within a cylindrical vessel was longer than that in a spherical one. Moreover, they reported that the proposed model could be effectively utilized to design latent thermal storage units.

Sridharan [72] investigated the impact of the aspect ratio on the thawing and freezing of PCM within a vertical cylindrical vessel computationally. The aspect ratio was defined as the height to the diameter of the capsule. The predicted results proved that the higher solidification time resulted from a small aspect ratio (or high Grashof numbers). Also, the velocity of natural convection currents decreased dramatically during freezing regardless of the aspect ratio. Therefore, the conduction mechanism was dominant during the freezing process.

Motahar and Khodabandeh [73] experimentally studied the influence of utilizing a heat pipe on the fusion and discharging features of n-octadecane paraffin in a vertical cylindrical storage unit placed within the reservoir of a constant-temperature bath. The test cell was a transparent acrylic glass tube with a height of 130

mm and a diameter of 25 mm. The experimental outcome pointed out that the freezing rate was substantially enhanced by utilizing the heat pipe. The transient movement of the solidification front on the surface of the heat pipe was photographically presented (Fig. 18). In addition, it was observed that a decrease of 10°C in the temperature of the reservoir reduced the solidification time by 49%.

Alexiadis et al. [74] developed a simulated model based-Smoothed Particle Hydrodynamics (SPH) method to evaluate both solidification and natural convection of multiple cases of PCM within a cylindrical pipe that its

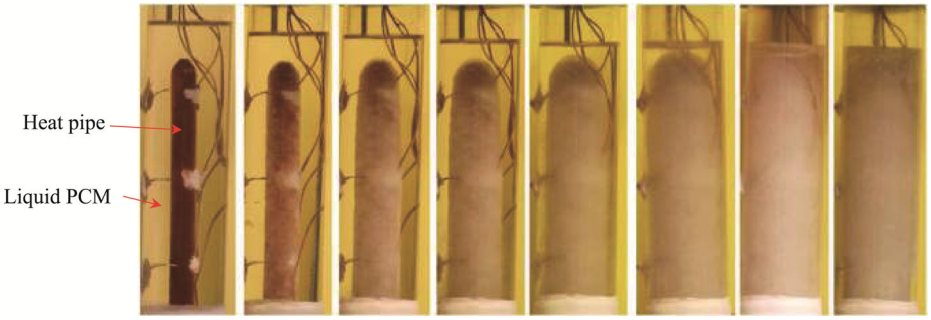


**Fig. 18** Evolution of the solid layer on the heat pipe during charging for a constant wall temperature of 5°C (Motahar and Khodabandeh [73])

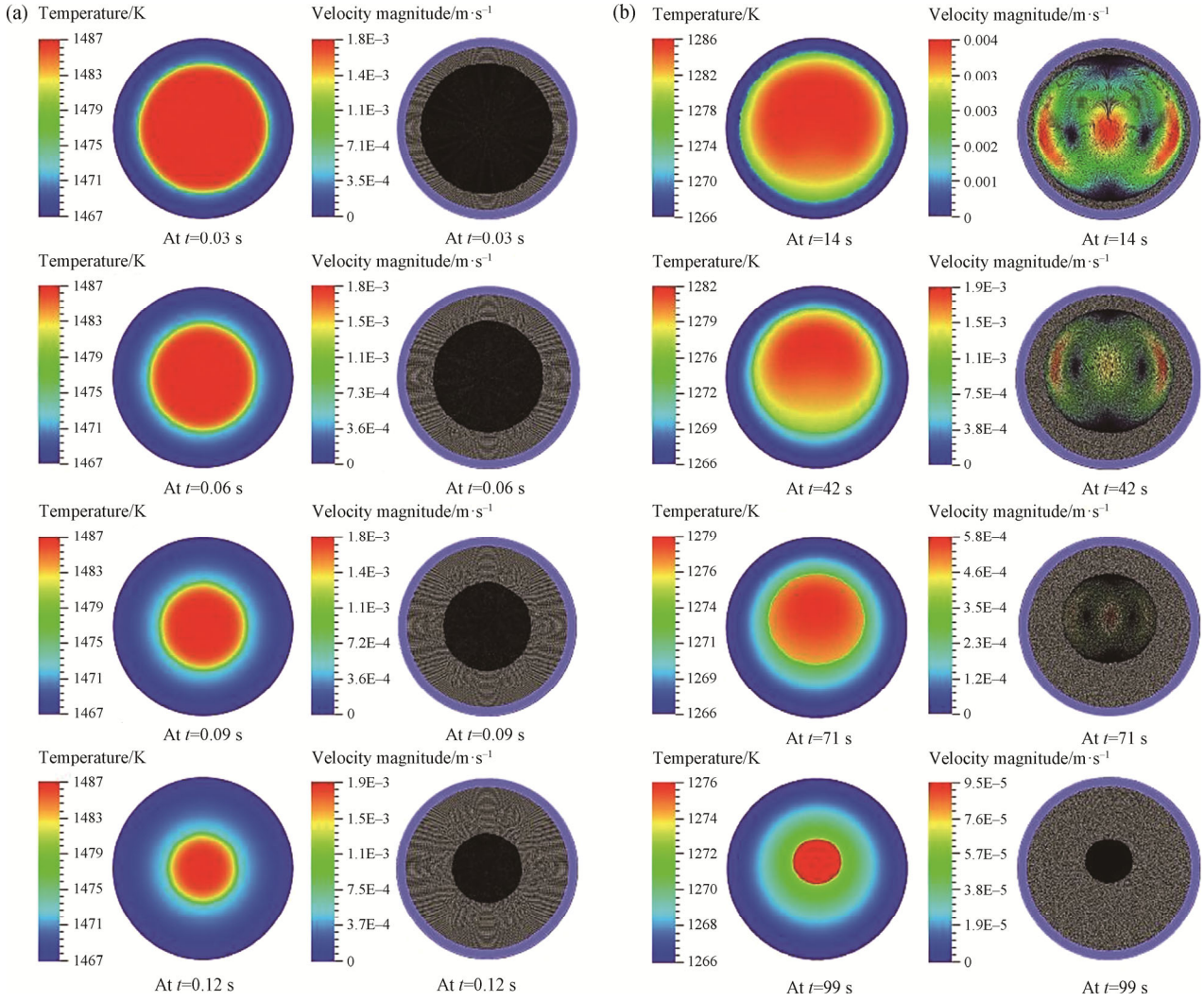


**Fig. 19** Temperature distributions and velocity vectors for (a) static regime and (b) dynamic regime (Alexiadis et al. [74])

walls were maintained at a constant temperature. It was shown that the PCM flow could be static, dynamic, or pseudo-static. In the case of the static regime, the effect of natural convection is minimal, and the freezing front moves axisymmetrically from the wall of the pipe to the center (Fig. 19(a)). In contrast, in the dynamic regime, buoyancy forces were developed due to density variation, and solidification does not grow symmetrically. The thicker solidified layer around the wall was observed in the bottom part of the pipe (Fig. 19(b)). Two competitive processes characterized the pseudo-static regime: a buoyancy-driven boundary layer and the advancing freezing front. As a result, solidification occurs faster than the time required for developing the buoyancy-driven boundary layer. Also, simple correlations were derived for predicting the solidification time of a given PCM.

Stamatiou et al. [75] presented the temperature-based approach combined with a quasi-stationary approximation model to describe the solidification of paraffin wax inside a vertical cylindrical tank. The five-loop tube carrying cooling HTF was inserted inside the tank. A test rig was also constructed to validate the simulated results. The predicted and experimental results of power output agreed well, which indicated the high accuracy of the model. Based on the fast and satisfying accurate results, it was reported that the developed model could be utilized effectively to design the heat storage unit.

Han et al. [76] experimentally examined the influences of the Stefan number, height and radius of the cylindrical cavity, and superheating factor on the final freezing configuration of PCM in a cylindrical cell. The cell had different radii (24–35.5 mm) and various heights (10–50 mm). Three morphologies (concave shape, Gaussian-distribution-like shape and the inside-hole shape) of solidified PCM were observed successively with the cavity height increasing. Also, the Stefan number strongly affected the final solidification of the PCM strongly, as shown in Fig. 20. In contrast, the superheating factor had a negligible impact on the final solidification shape.


**Fig. 20** The final shapes of solidified PCM for different Stefan numbers (Han et al. [76])

Izgi and Arslan [77] developed a three-dimensional model to assess the different factors in the discharging process of PCM encapsulated within a vertical cylindrical cavity. The effect of the natural convection was involved in the computational model. The cavity was exposed to a convective cooling environment. It was observed that the natural convection role was significant during the freezing process's early duration. Then, the conduction mechanism dominated the entire process. Also, the cavity diameter had an important impact on the freezing process, while the influence of cavity height was not noticeable.

Olfian et al. [78] computationally researched the effect of employing a corrugated U-tube on the thermal characteristics of an evacuated tube solar collector (ETSC)-integrated PCM (Fig. 21) during charging and discharging modes. In all cases, the corrugated tube system exhibited higher performance than the smooth tube system. The influences of geometric parameters (corrugation depth and pitch and a number of lobes) on the thermal behaviour of the system were assessed. The system's daily operation was enhanced due to the extension in the time of discharging process at night. Among all geometric parameters, the number of lobes had the greatest influence on thermal performance.

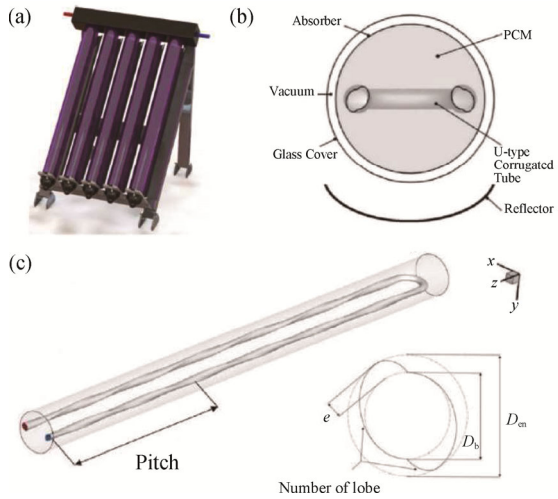


**Fig. 21** Schematics diagrams of (a) ETSC, (b) ETSC-integrated PCM, and (c) U-corrugated tube (Olfian et al. [78])

A summary of the studies devoted to the discharging of PCM in cylindrical cavities is presented in Table 3. From the above literature, it is concluded that the cylindrical cavity's size greatly impacts the discharging process. Still, the diameter of the cavity has a more significant effect than that of the height of the cavity. Also, the flow rate and temperature of flowing HTF affect the discharging process.

**Table 3** Summary of investigations on PCM discharging in cylindrical enclosures

| Authors (Year) | Configuration and Conditions | PCM ($T_m$) | Type of Study | Highlighted Results/Findings |
|---|---|---|---|---|
| Bilir and Ilken [68] (2005) | Freezing in a constant surface vessel | Water (0°C, NA) | Numerical (CVA) | The resulting correlations were reliable and could be used in many engineering applications with high accuracy. |
| Kalaiselvam et al. [69] (2007) | Solidification and melting inside storage cell cooled by water bath | 60% n-tetradecane + 40% n-hexadecane (5°C, 0.146–0.34 W/(m·K)), n-tetradecane (5.5°C, 0.15–0.35 W/(m·K)), and n-pentadecane (9.6°C, 0.15–0.182 W/(m·K)) | Analytical (conduction model, and conduction and heat generation model) and Experimental | The model considering the conduction and heat generation was more accurate in predicting the freezing front. The predictions proved that the freezing time varies positively with the Stefan number and inversely with the heat generation parameter. The 60% n-tetradecane + 40% n-hexadecane mixture PCM indicated more excellent phase-change characteristics than the two other kinds of PCM. |
| Lu et al. [70] (2010) | Solidification/melting inside a horizontal pipe during the cold filling process of PCM | Molten salt (137–142°C, 0.571 W/(m·K)) | Numerical (VOF, continuum surface force model) | The maximum thickness of solidified layer caused a maximum flow velocity. The boundary heat flux increased in the solidification process. |
| Rajeev and Das [71] (2010) | Horizontal cylindrical and spherical cavities at a uniform wall temperature | A dimensionless study, general type PCM (NA, NA) | Numerical (1-D conduction model) | The velocity of the solid-liquid interface decreases with the Stefan number. For the same Stefan number, the solidification time of PCM inside a cylindrical container was longer than that in a spherical one. |
| Sridharan [72] (2013) | Thawing and freezing inside vertical vessel subjected to an isothermal boundary condition | Sodium nitrate (304.95–306.95°C, temperature-dependent) | Numerical (VOF, EPM, FVM) | Higher solidification time resulted from a small aspect ratio (or high Grashof numbers). The role of natural convection was suppressed dramatically during freezing regardless of the aspect ratio. |
| Motahar and Khodabandeh [73] (2016) | Vertical vessel with heat pipe placed in the constant-temperature reservoir | Octadecane (28°C, 0.2 W/(m·K)) | Experimental | The solidification rate was substantially enhanced by utilizing the heat pipe. The reduction in solidification time was 49% due to a 10°C decrease in the temperature of the reservoir. |
| Alexiadis et al. [74] (2018) | Horizontal pipe at a uniform wall temperature | Multi-types of PCM | Numerical (Smoothed Particle Hydrodynamics method) | Three flow regimes were identified: static, dynamic, and pseudo-static. The correlations for predicting the freezing time were derived. |
| Stamatiou et al. [75] (2018) | Vertical cylindrical container with cooling HTF inside the tube with multi loops | RT10 (9.2°C, 0.18–0.2 W/(m·K)) | Experimental and Numerical (the temperature-based approach combined with the quasi-stationary approximation model) | According to the accurate results and low computational complexity, the model can be applied efficiently to design latent heat storage systems. |
| Han et al. [76] (2019) | Solidification inside cavity exposed to air room at a constant temperature | RT60 (55–61°C, 0.2 W/(m·K)) | Experimental | Both the Stefan number and the cavity's height had a significant effect on the final shape of solidification, while the superheating factor did not. |
| Izgi and Arslan [77] (2020) | Solidification of PCM inside vertical tube due to convective cooling environment | Paraffin wax RT50 (45–51°C, 0.2 W/(m·K)) | Numerical (EPM, FVM) | The natural convection role was significant only at the early duration of the freezing process. The influence of the cavity diameter was more significant than that of cavity height on the solidification process. |
| Olfian et al. [78] (2021) | Charging/discharging in evacuated tube solar collector with U-corrugated tube | Paraffin wax (54–57°C, 0.21 W/(m·K)) | Numerical (EPM, FVM) | Utilizing the corrugated tube enhanced the thermal performance of the system. The lob number had the most influence on thermal performance. |

## 5. Discharging of PCM in Annular Heat Storage Units

In most annular storage units, the heat transfer fluid (HTF) passes through an inner tube, whilst the PCM is contained inside the annular space between the inner tube and outer shell. This configuration of PCM container can be effectively used as a heat exchanger due to its simple structure, higher thermal performance, minimum volume of PCM, and lower heat losses [79, 80]. The annular heat storage unit can be positioned vertically or horizontally.

Trp [81] examined transient thermal characteristics of charging and discharging in the annular cell experimentally and numerically. The water flowed in the internal tube as HTF, while the technical grade paraffin was enclosed inside the shell-and-tube space, as described in Fig. 22. The test unit was composed of two concentric tubes. The diameter of the copper inner tube was 0.035 m, while the brass outer tube had a diameter of 0.128 m. A reasonable agreement was observed between predictions and experimental findings for isothermal solidification. Also, it was reported that the numerical solution could be used effectively to provide the thermal performance and design optimization of the LHTES.

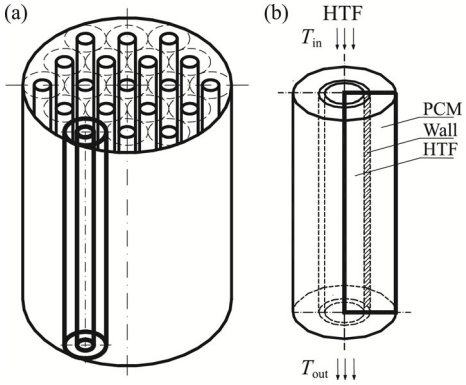


**Fig. 22** Latent thermal energy storage system, and thermal energy storage unit (Trp [81])

Jian-you et al. [82] evaluated computationally and experimentally the charging and discharging processes in triplex concentric tubes. The inner tube's length and diameter were 3100 and 15 mm. The middle tube had an inner diameter of 80 mm and a length of 3000 mm. Also, the length and inner diameter of the outer tube were 3040 and 90 mm, respectively. The PCM was filled in the middle channel, with hot HTF flowing in the outer channel during the charging process and cold HTF flowing in the inner channel during the discharging process (Fig. 23). The numerical analysis considered that the conduction dominated the phase-change process. The reasonable agreement between numerical and experimental results led to the possibility of accurately using the numerical approach for designing and evaluating the LHTES systems' thermal performance.

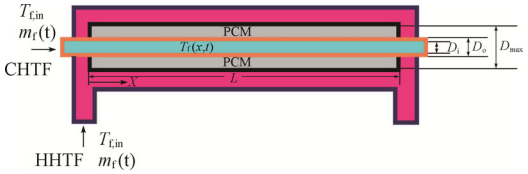


**Fig. 23** Schematic configuration of LHTES unit (Jian-you et al. [82])

Ezan et al. [83] estimated the influence of different geometric and operating conditions (shell size, tube material, flow rate and inlet temperature of HTF) on the thawing and freezing of water held in the annular space of a horizontal heat exchanger experimentally. The radii of the inside and the outside of the inner tube were 15 and 25 mm, respectively. The solid-liquid interface was monitored by an electronic ice thickness measurement method. The findings indicated that the inlet HTF temperature significantly influenced the solidification process, among other parameters.

Lipnicki and Weigand [84] presented a theoretical model and experimental study to prove the significant influence of the contact layer between a cooled wall and solidified water on the solidification process in a vertical annular cavity. The inner tube diameter, outer tube diameter, and height of the annular channel were 134, 200, and 170 mm, respectively. It was shown that the growth rate of the frozen layer was slow, and the thermal resistance of the contact layer was time-dependent at the beginning of discharging process. At later time instants, quick growth of a solidified layer of ice was observed. Also, the thermal resistance of the contact layer can be deemed constant for longer time.

Longeon et al. [85] experimentally and numerically studied the thawing and freezing of RT35-PCM in a vertical annular storage unit. The inner steel tube diameter of 15 mm and the outer Plexiglas shell of a diameter of 44 mm formed the annular cavity of PCM. The influence of HTF injection configurations (top and bottom) inside the inner tube was assessed. The results indicated that the freezing interface travels upward with an oblique shape (Fig. 24), and the influence of natural convection was insignificant during the discharging process. Moreover, a bottom injection of HTF was recommended for discharging process because the PCM solidified first at the bottom of the unit, and liquid PCM could refill the voids.

Avci and Yazici [86] explored the charging and discharging of paraffin in the horizontal annular cavity of a shell and tube storage unit experimentally. A 3.3 kg of PCM filled the annular space formed between an inner copper tube of 28 mm in diameter and a polypropylene

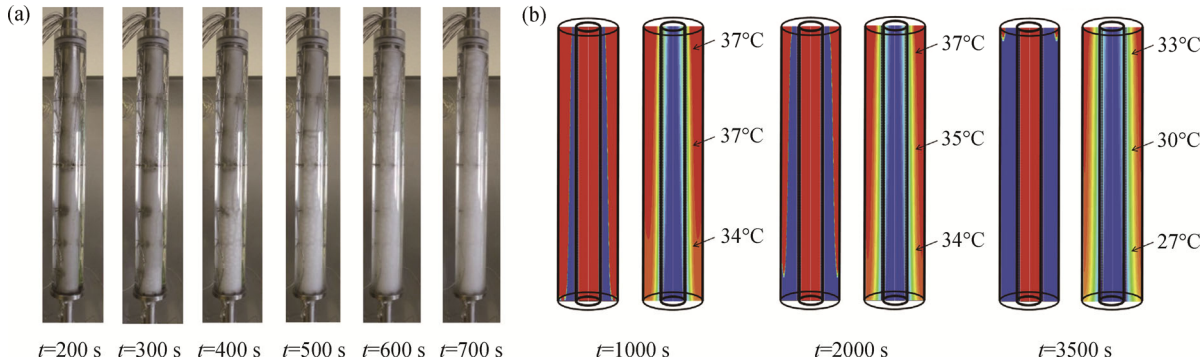


**Fig. 24** (top) Photographs of experimental transient progress of the liquid fraction, (bottom) Numerical liquid fractions and temperature distribution during solidification process with bottom injection of HTF (Longeon et al. [85])

shell of 110 mm in diameter. The time-variation of the PCM temperature field was measured to evaluate the phase-change processes. The experimental findings showed an abrupt variation in the temperature of PCM during the beginning of the discharging process due to the large temperature difference between HTF and paraffin. The natural convection was effective initially; however, the conduction mechanism dominated the solidification process at later instants. Moreover, decreasing the inlet temperature of HTF accelerated the discharging process, as indicated in Fig. 25.

Solomon et al. [87] offered an experimental investigation to inspect the influence of subcooling on the outward solidification of RT-21 PCM contained in the annulus of a vertical double pipe heat exchanger. The air, as cooling HTF, flowed through the inner tube of 75 mm in diameter. The shell was made from acrylic 140 mm in diameter. It was noticed that the highest cooling rate was near the entry zone of the HTF stream. Also, the increase in the subcooling effect and a decrease in the solidification temperature of the PCM resulted in a higher cooling rate. Further, it was observed that increasing the inlet velocity of air beyond a certain value had a negligible impact on the solidification process for the high-temperature difference between the PCM and the HTF.

Jesumathy et al. [88] conducted experimental work to explore the influences of operating conditions of HTF on the thawing and discharging of PCM in a horizontal double pipe heat exchanger. The paraffin wax was contained between an inner brass tube of 43 mm in diameter and an outer shell of 98 mm in diameter. The outcomes pointed out that the mechanism of heat conduction dominated the solidification process. Also, the operating conditions of the HTF had a more pronounced effect on the charging process compared to their influence on the discharging process.

Hosseini et al. [89] performed an experimental and computational study to examine the characteristics of charging and discharging of RT50-PCM in a horizontal shell and tube heat exchanger. The diameters of the shell

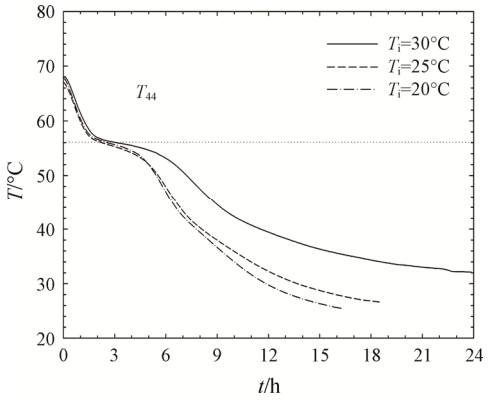


**Fig. 25** Temporal variations of PCM temperature near the shell surface as registered by thermocouple ($T_{44}$) at different inlet temperatures ($T_i$) of HTF (Avci and Yazici [86])

and tube were 85 and 22 mm, respectively. They defined the theoretical efficiency of the heat exchanger, which measured the sufficiency of exchanged energy between PCM and HTF for completing the phase-change conversion. It was found that HTF temperature had less effect on the solidification process. Raising the HTF temperature from 70°C to 80°C only increased the theoretical efficiency of the solidification process from 79.7% to 81.4%.

Ismail et al. [90] introduced a numerical investigation supported and validated by experimental findings to study the solidification of PCM (water) along a horizontal tube inside the insulated shell. The simulations utilized the boundary immobilization technique. Good agreements were achieved between predicted results and experimental data of the model on one side and between predicated results and numerical findings of the literature on another side. They reported that this validation and agreement confirmed that the immobilization technique could be used reliably to solve phase change problems. Also, the temperature of HTF had a marked impact, whereas the flow rate of HTF had a moderate impact on the solid-liquid interface position and velocity, the solidified fraction, and the solidification time.

Kibria et al. [91] computationally and experimentally researched the discharging and charging of paraffin wax in an annular heat exchanger. The inner diameters of the tube and shell were 10.8 and 36.0 mm, respectively. The computational investigation depended on the iteration of the temperature and thermal resistance model. The results revealed that the inlet HTF temperature and radius of the internal tube had a stronger influence on the solidification process than the flow rate of HTF and thickness of the tube.

Yazici et al. [92] experimentally investigated the impact of the eccentricity in a horizontal tube-in-shell thermal energy storage system on the discharging behaviour of paraffin PCM. The eccentricity (either upward or downward) was generated as the centers of the inner tube, and the outer shell did not coincide. The eccentricity values ranged from –30 mm to 30 mm. The cold heat transfer fluid (water) flowed inside the inner tube diameter of 28 mm, while the outer shell of diameter of 100 mm was thermally insulated. It was found that both upward and downward eccentricity prolonged the solidification time. Therefore, the concentric mode should be favoured to attain improved performance of PCM solidification.

Bechiri and Mansouri [93] developed an analytical model to conduct a parametric study of thawing and freezing in an annular TES unit. The influences of the HTF flow rate, storage unit length, and tube radius on the features of phase change processes were evaluated. The model was validated by comparing the analytical results with the experimental and numerical results found in the literature. A dramatic decrease in PCM temperature was indicated at the first stage of solidification. Then, this decrease was more gradual at later time instants since the conduction mechanism dominated the solidification process. Also, it was reported that the analytical model presented a reasonable estimation of the thermal performance of charging and discharging processes.

Agarwal and Sarviya [94] carried out experiments on the fusion and freezing of PCM in a horizontal annular TES unit, which can be utilized as a component of solar food dryer systems. Air was used as the HTF in an internal tube with a diameter of 25 mm. Also, the external shell had a diameter of 127 mm. It was found that the discharging of PCM was controlled by conduction, and a high solidification rate was observed during the initial time instants. Also, higher flow rates of the HTF led to the largest cumulative discharged energy and a decrease in discharging time. Moreover, it was inferred that the latent heat storage unit could provide the required hot air for drying food products during periods of low-intensity solar energy.

Seddegh et al. [95] investigated and compared numerically the thermal characteristics of charging and discharging processes in both vertical and horizontal annular TES units. Conduction and convection heat transfer mechanisms were considered for both processes. The HTF flowed within the inner tube, while the paraffin wax-PCM was contained in the annular space between the outer shell and the inner tube. The predicted results of the model-based enthalpy method were validated utilizing published experimental findings. The simulated results indicated that the conduction mechanism dominated the discharging process. The same discharging rate was recorded in both orientations of the energy storage unit (Fig. 26). This behaviour was fundamentally due to the lower thermal conductivity of the PCM, which slowed down the discharging process for both systems. Also, it was found that the HTF flow rate had an insignificant effect on both the charging and solidification processes.

Wang et al. [96] experimentally examined the thawing and freezing of erythritol-PCM in a vertical annular cavity. The air as the HTF flowed from top to bottom of the internal tube with 40 mm in diameter. It was deduced that the erythritol solidified from the lower region initially, and then the freezing front advanced uniformly and externally from the tube towards the outer shell of 100 mm in diameter. Also, the natural convection mechanism dominated only the initial periods of the discharging process. Moreover, the thermal performance of discharging process was enhanced by increasing the flow rate of the HTF.

Ma et al. [97] simulated the discharging process and the phase change of the supercooled sodium acetate (SA) aqueous solution to sodium acetate trihydrate in a shell-and-tube heat exchanger. The PCM was contained inside the shell, while the HTF flowed within the internal tube. The thermophysical properties of SA were modelled and calculated at different concentrations and temperatures. The simulation results showed that the discharging process was quick initially due to the deep subcooling of SA. Then, the charging proceeded slowly and was dominated by the diffusion heat transfer. Also, increasing the flow rate of HTF caused a higher thermal power output; however, this was not favourable for seasonal solar TES.

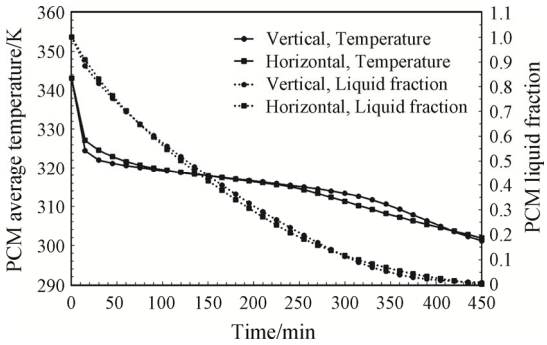


**Fig. 26** Average temperature and liquid fraction of PCM during discharging process for two orientations of the storage unit (Seddegh et al. [95])

Riahi et al. [98] simulated the effect of the periodic boundary condition on the fusion and freezing processes inside a vertical annular storage system. The direction of inlet HTF was periodically reversed. The predictions showed higher heat transfer rates and more uniform temperatures were indicated for both processes when periodic boundary conditions were imposed compared to fixed boundary conditions. In addition, for the case of periodic boundary conditions, the solidification time was 12% faster than that of fixed boundary conditions. The same authors [99] studied the effect of HTF flow configurations in the tube on charging and discharging in horizontal and vertical shell and tube heat exchangers numerically. The flow configurations were symmetric parallel flow SPF (one tube of HTF), parallel flow PF (parallel HTF in all tubes), and counter flow CF (HTF passes in two tubes in series), as described in Fig. 27. For both processes, the predicted findings exhibited that the vertical PF configuration showed improved effectiveness and lower uniformity of the phase-change process than that experienced by the vertical CF heat exchanger. Also, a minor influence of heat exchanger orientation was observed on the solidification process.

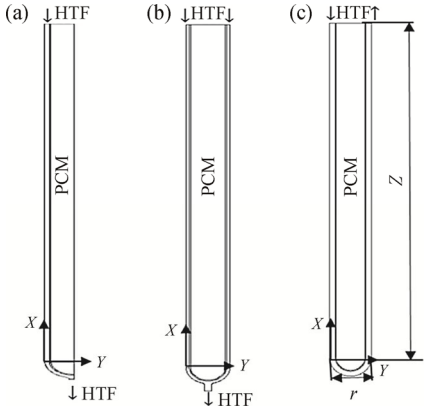


**Fig. 27** Configuration of HTF flow: (a) SPF, (b) PF, (c) CF (Riahi et al. [99])

Tao et al. [100] presented a 3-D model to explore the influence of considering natural convection and PCM arrangements on the charging and discharging of PCM in shell and tube latent heat storage units. The PCM was contained in tube side arrangement and in shell side arrangement. The predicted results exhibited that the PCM-in-tube arrangement enhanced the heat storage significantly compared with the PCM-in-shell layout for the same geometry and operation conditions. In addition, little impact of natural convection was observed on the thermal behaviour of the discharging process.

Elmeriah et al. [101] numerically explored the influence of geometric and operating conditions on the discharging and melting of paraffin wax in a horizontal annular storage unit. The influences of shell diameter, tube length and the Reynolds number of the HTF were assessed. The results showed that the geometric parameters (shell diameter and tube length) had a significant impact on the outlet HTF temperature. At the same time, the Reynolds number affected the charging and discharging rates. Moreover, using two layers of PCM (RT60 and paraffin wax) improved the performance of the storage unit compared to the unit having only one layer of PCM (paraffin wax).

Tehrani et al. [102] assessed numerically the geometric and operating conditions under which the buoyancy-driven convection is worthy or not to consider in a numerical model to investigate the charging and discharging in high-temperature vertical annular latent TES units. For all studied cases, the maximum errors of considering the pure-conduction model instead of the convection model are higher for melting compared with the solidification (100% in melting versus 30% in solidification). Also, the error increased with the decrease of the tube length and increase of the radius ratio (shell radius to pipe radius). Furthermore, the error depended on the dimensionless groups, the ratio of pipe radius to unit length, and the Biot, the Rayleigh and the Stefan numbers. However, it was found that the Rayleigh number had a greater influence than other groups. The error of omitting natural convection was less than 1% when the Rayleigh number was lower than its critical value of $8\times10^5$.

Mehta et al. [103] presented a computational and experimental inspection to examine the fusion and freezing of stearic acid-PCM in horizontal and vertical latent thermal storage cells. The inner diameters of the brass tube and stainless steel shell were 28 and 88 mm, respectively. It was reported that except for the initial period of discharging when natural convection dominated, the conduction mechanism controlled the entire solidification process. In addition, the influence of the storage unit orientation seemed to be small on the thermal performance of the solidification process (Fig. 28).

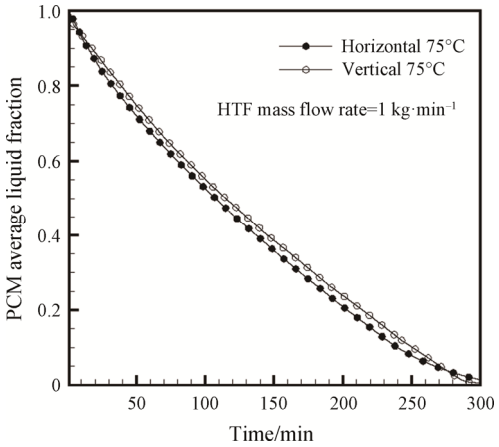


**Fig. 28** Instantaneous liquid fraction during solidification in horizontal and vertical storage units (Mehta et al. [103])

**Table 4** Summary of works on PCM discharging in annular TES units

| Authors (Year) | Configuration and Conditions | PCM ($T_m$) | Type of Study | Highlighted Results/Findings |
|---|---|---|---|---|
| Trp [81] (2005) | Melting and solidification in a vertical storage unit | Technical grade paraffin (27.7°C, 0.18–0.19 W/(m·K)) | Experimental and Numerical (CVA) | The numerical solution could provide the thermal performance and design optimization of the LHTES system. |
| Jian-you et al. [82] (2008) | Charging and discharging in a triplex shell-and-tube thermal storage unit | N-Hexacosane (56.3°C, 0.22 W/(m·K)) | Experimental and Numerical (temperature and thermal resistance iteration method) | The numerical simulation could accurately evaluate the LHTES system's performance and provide design optimization. |
| Ezan et al. [83] (2011) | Melting/solidification in a horizontal heat exchanger | Water (°C, NA) | Experimental | Inlet HTF temperature had a significant influence on the solidification process, among other parameters. |
| Lipnicki and Weigand [84] (2012) | The influence of the contact layer on the solidification in a vertical annular cavity | Water (0°C, NA) | Experimental and theoretical | Growth of the frozen layer was slow at the beginning of discharging process, and then it developed quickly. The thermal resistance of the contact layer can be deemed constant for later time. |
| Longeon et al. [85] (2012) | Charging/discharging PCM in a vertical cavity for two injection methods of HTF from top and bottom | RT35 (35°C, 0.2 W/(m·K)) | Experimental | The impact of free convection was insignificant during the discharging process. A bottom injection of HTF was recommended for discharging process. |
| Avci and Yazici [86] (2013) | Melting and solidification in a horizontal unit | Paraffin wax (56–58°C, NA) | Experimental | Natural convection was effective only during the initial period of the solidification process. Decreasing the inlet temperature of HTF accelerated the solidification process. |
| Solomon et al. [87] (2013) | Vertical heat exchanger with cooling air in the inner tube | RT21 (19–22°C, 0.2 W/(m·K)) | Experimental | The highest cooling rate was near the entry zone of HTF. A higher cooling rate resulted from increasing the subcooling effect and decreasing the solidification temperature. |
| Jesumathy et al. [88] (2014) | Horizontal double pipe storage unit | Paraffin wax (58–60°C, 0.15–0.24 W/(m·K)) | Experimental | The operating conditions of HTF affected the melting process more highly than the solidification process. |
| Hosseini et al. [89] (2014) | Charging/discharging in a horizontal heat exchanger | Paraffin wax (50°C, NA) | Experimental and Numerical (EPM, FVM) | The temperature of HTF had less impact on the freezing process. |
| Ismail et al. [90] (2014) | The solidification of the PCM layer was along with the array of tube surfaces through which the cold refrigerant flows. | Water (0°C, 0.6 W/(m·K)) | Experimental and Numerical (boundary immobilization technique) | The influences of temperature and flow rate of HTF are strong and moderate, respectively, on the solid-liquid interface position and velocity, the solidified fraction, and the solidification time. |
| Kibria et al. [91] (2014) | Charging and discharging in a horizontal storage unit | Paraffin wax (61°C, 0.2–0.22 W/(m·K)) | Experimental and Numerical (iteration of temperature and thermal resistance model) | The inlet HTF temperature and radius of the internal tube influenced the solidification process highly compared to the flow rate of HTF and tube thickness. |
| Yazici et al. [92] (2014) | Eccentric and concentric horizontal annular storage unit with discharged by cold water | Paraffin (56–58°C, NA) | Experimental | Upward and downward eccentricity resulted in an extension of solidification time. |
| Bechiri and Mansouri [93] (2015) | Fusion and freezing in a horizontal storage cell | Technical grade paraffin (27°C, 0.18 W/(m·K)) | Analytical (Exponential Integral Function) | A dramatic decrease in PCM temperature and the effective role of natural convection was indicated at the first stage of solidification. |
| Agarwal and Sarviya [94] (2016) | Charging and discharging in a horizontal heat exchanger | Paraffin wax (41–55°C, 0.21 W/(m·K)) | Experimental | The discharging of PCM was controlled by conduction. The HTF flow rate had a substantial impact on the discharged energy and discharging time. |

**(Continued Table 4)**

| Authors (Year) | Configuration and Conditions | PCM ($T_m$) | Type of Study | Highlighted Results/Findings |
|---|---|---|---|---|
| Seddegh et al. [95] (2016) | Charging and discharging in horizontal and vertical shell and tube storage unit | RT-50 (45–51°C, 0.2 W/(m·K)) | Numerical (EP, FVM) | No effect of storage orientation was recorded on the discharging rate.<br>The flow rate of HTF has an insignificant effect on both melting and solidification. |
| Wang et al. [96] (2016) | Charging and discharging of PCM in a vertical cavity where air (HTF) flowed from top to bottom | Erythritol (120.39°C, 0.68–0.76 W/(m·K)) | Experimental | PCM started solidification from the lower region, and then it advanced uniformly and externally from the tube towards the shell. |
| Ma et al. [97] (2017) | Discharging of large supercooling-degree PCM in the vertical heat exchanger | Sodium acetate (SA) aqueous solution (58°C, 0.453–0.7 W/(m·K)) | Numerical (CVA, FDM) | Initially, the discharging process was quick due to the deep subcooling of SA. Then, the charging proceeded slowly and was dominated by the heat transfer conditions. |
| Riahi et al. [98] (2017) | Melting and solidification in shell and tubes unit where the inlet flow of HTF was periodically reversed to attain periodic boundary conditions | Sodium nitrate (306.8°C, NA) | Numerical (EPM, FVM) | Higher thermal performance was achieved when periodic boundary conditions were imposed instead of fixed boundary conditions.<br>Solidification time under periodic boundary conditions was 12% faster than that of fixed boundary conditions. |
| Riahi et al. [99] (2017) | Charging and discharging in two orientations of the heat exchanger and various configurations of HTF flow | Sodium nitrate (306.8°C, NA) | Numerical (EPM, FVM) | Vertical PF showed a higher thermal performance than vertical CF heat exchangers.<br>A minor impact of heat exchanger orientation was observed on the solidification process. |
| Tao et al. [100] (2017) | Charging and discharging of PCM in two arrangements (in-tube and in-shell) with and without considering the impact of natural convection | LiF/$CaF_2$ (767°C, 3.8 W/(m·K)) | Numerical (EPM, FVM) | Using a PCM-in-tube arrangement enhanced heat storage significantly.<br>A little impact of natural convection on the thermal performance of discharging process was observed. |
| Elmeriah et al. [101] (2018) | Charging and discharging in horizontal annular unit | Paraffin wax (61°C, 0.228–0.24 W/(m·K)) and RT60 (57°C, 0.2 W/(m·K)) | Numerical (EPM, FVM) | Shell diameter and tube length had a significant impact on the outlet temperature of HTF, while the Reynolds number affected the charging and discharging rates.<br>Using two different PCMs achieve higher performance than utilizing one PCM. |
| Tehrani et al. [102] (2018) | Charging and discharging in the vertical annular unit to assess the error generated from considering and neglecting natural convection | H325 (325°C, 0.549 W/(m·K)), H425 (425°C, 0.565 W/(m·K)) and H525 (525°C, 0.565 W/(m·K)) | Numerical (EPM, FVM) | Neglecting natural convection affected the charging process highly compared with its effect on discharging process.<br>The error of disregarding natural convection in the numerical model depended on the dimensionless groups, i.e. geometry ratio, Rayleigh, Stefan and Biot numbers. |
| Mehta et al. [103] (2019) | Charging and discharging in a storage cell of two orientations | Stearic acid (55.7–56.6°C, 0.172–0.3 W/(m·K)) | Experimental and Numerical (EPM, FVM) | Orientation had a small influence on the solidification process. |
| Sodhi et al. [104] (2019) | Melting and solidification in a horizontal cylindrical and conical shells heat exchanger | Sodium nitrate (306°C, 0.495–0.565 W/(m·K)) | Numerical (Effective heat capacity approach, FEM) | The conical shell design enhanced the discharging process.<br>The discharging rate was enhanced by increasing the velocity of HTF and decreasing the inlet temperature of HTF. |
| Andrzejczyk et al. [105] (2020) | Thawing and freezing in a vertical heat exchanger with three configurations of the internal tube | Coconut oil (NA, NA) | Experimental | The top-coiled tube configuration achieved the best solidification performance.<br>The convection role was crucial in the solidification process of coiled tube configuration. |

Sodhi et al. [104] established a numerical model to evaluate sodium nitrate-PCM's charging and freezing features in conventional and modified horizontal latent heat storage units. The traditional unit contained a cylindrical shell, whereas the modified design had a conical shell (Fig. 29). The predictions pointed out that the conical shell design enhanced both the discharging and charging processes. The maximum decrease in discharging time was 28%. The discharging rate increased highly when the velocity of the HTF varied from 2 to 6 m/s, but the enhancement in this rate was significant beyond 6 m/s. Also, the inlet HTF temperature affected the discharging time markedly.

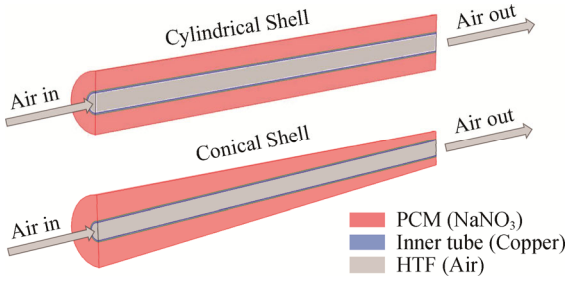


**Fig. 29** Cylindrical shell storage unit and conical shell unit (Sodhi et al. [104])

Andrzejczyk et al. [105] conducted experimental work to explore the charging and discharging of coconut oil-PCM in a vertical annular TES unit formed from an internal helical coil of 10 mm diameter and an outer shell of 50 mm diameter. Three configurations of internal tube geometry were considered: the straight tube, the top-coiled tube, which comprised the helical section at the top, accompanied by a straight tube, and the bottom-coiled tube, in which the helical section is at the bottom. The experimental findings suggested that the top-coiled tube configuration achieved the most improved solidification performance. Also, the role of convection was crucial in the solidification process of two types of coiled tubes, while this role dominates only the initial duration of the solidification process in the conventional straight-tube case.

A summary of the studies devoted to the discharging of PCM in annular TES units is presented in Table 4. The results of the above literature indicate that the size of the annular cavity and the HTF's inlet temperature greatly affect the discharging process. Also, the eccentricity of the horizontal annular cavity and the bottom injection of HTF in the vertical cavity is favourable for discharging process.

## 6. Conclusions

The solidification features of PCM in multiple-shape thermal storage containers are reported and reviewed. The considered containers are planar, spherical, cylindrical and annular thermal storage systems. For all cavities, the buoyancy-driven convection dominates only the early duration of the freezing process. As time travels, the conduction is a privilege of the entire process. Therefore, the solidification rate is higher at the initial periods of the solidification process. Also, decreasing the temperature and increasing the flow rate of cooling HTF reduced freezing time. However, the influence of HTF temperature is more significant than that of HTF flow rate. Moreover, the impact of the initial superheating is insignificant. On the other hand, the container's size plays an essential role in the discharging process. An increase in the container's size is accompanied by the increased amount of involved PCM and an extension of freezing duration. In addition, the aspect ratio of the cavity affects the freezing behaviour inside planar and vertical cylindrical cells. Moreover, the cavity orientation (horizontal and vertical) has a minor effect on the solidification inside annular cavities.

## 7. Challenges, Anticipation, and Proposals for Future Studies

The main challenges of developing PCM applications in LHTESS (latent heat thermal energy storage system) are inherent properties and phenomena such as low-thermal conductivity, supercooling, cycling degradation, instability, hysteresis, etc. The low thermal conductivity of PCM can be fixed by many enhancement methods, like fins involvement, porous media insertion, and nanoparticle dispersion within PCM. The effects of these methods were well-documented in the literature. On the other hand, supercooling means that the liquid PCM does not crystallize or solidify even if it is cooled lower than solidus temperature. Some PCMs suffer from various levels of supercooling problems, which are assumed negligible in most numerical investigations and thus affect the accuracy of predictions. However, the supercooling effect can be controlled practically by adding additives, varying the characteristics of PCM containers and controlling the cooling rate.

The hysteresis between the charging and discharging process imposes some limitations on the applications of LHTESS in various fields. The hysteresis has resulted from inappropriate measurement methods to evaluate the PCM and their intrinsic material properties. Thus, it is more important to consider PCM temperature hysteresis in numerical models to obtain more accurate results. Also, the other challenges, such as performance degradation of PCM and its instability during charging-discharging cycles, should be considered for long-term investigation of LHTESS.

## References


[1] Ye W.B., Li C., Huang S.M., Hong Y., Validation of thermal modeling of unsteady heat source generated in a rectangular lithium-ion power battery. Heat Transfer Research, 2019, 50(3): 233–241. https://doi.org/10.1615/HeatTransRes.2018026809.

[2] Ye W.B., Li C., Gong S., Hong Y., Huang S.M., Xu S., Study on thermal uniformity and improvement for the drying of lithium-ion batteries. International Journal of Fluid Mechanics Research, 2019, 46(6): 487–498. https://doi.org/10.1615/InterJFluidMechRes.2019027012.

[3] Yang X., Guo J., Yang B., Cheng H., Wei P., He Y.L., Design of non-uniformly distributed annular fins for a shell-and-tube thermal energy storage unit. Applied Energy, 2020, 279: 115772. https://doi.org/10.1016/j.apenergy.2020.115772.

[4] Wang X., Li W., Luo Z., Wang K., Shah S.P., A critical review on phase change materials (PCM) for sustainable and energy efficient building: Design, characteristic, performance and application. Energy & Buildings, 2022, 260: 111923. https://doi.org/10.1016/j.enbuild.2022.111923.

[5] Hua W., Zhang L., Zhang X., Research on passive cooling of electronic chips based on PCM: A review. Journal of Molecular Liquids, 2021, 340: 117183. https://doi.org/10.1016/j.molliq.2021.117183.

[6] Fan L., Khodadadi J.M., Thermal conductivity enhancement of phase change materials for thermal energy storage: A review. Renewable and Sustainable Energy Reviews, 2011, 15(1): 24–46. https://doi.org/10.1016/j.rser.2010.08.007.

[7] Dhaidan N.S., Khodadadi J.M., Improved performance of latent heat energy storage systems utilizing high thermal conductivity fins: A review. Journal of Renewable and Sustainable Energy, 2017, 9(3): 034103. https://doi.org/10.1063/1.4989738.

[8] Guo J., Du Z., Liu G., Yang X., Li M.J., Compression effect of metal foam on melting phase change in a shell-and-tube unit. Applied Thermal Engineering, 2022, 206: 118124. https://doi.org/10.1016/j.applthermaleng.2022.118124.

[9] Dhaidan N.S., Nanostructures assisted melting of phase change materials in various cavities. Applied Thermal Engineering, 2017, 111: 193–212. http://dx.doi.org/10.1016/j.applthermaleng.2016.09.093.

[10] Dhaidan N.S., Kokz S.A., Rashid F.L., Hussein A.K., Younis O., Al-Mousawi F.N., Review of solidification of phase change materials dispersed with nanoparticles in different containers. Journal of Energy Storage, 2022, 51: 104271. https://doi.org/10.1016/j.est.2022.104271.

[11] Jain S., Kumar K.R., Rakshit D., Heat transfer augmentation in single and multiple (cascade) phase change materials based thermal energy storage: Research progress, challenges, and recommendations. Sustainable Energy Technologies and Assessments, 2021, 48: 101633. https://doi.org/10.1016/j.seta.2021.101633.

[12] Dhaidan N.S., AL-Jethelah M., Study on the effect of nanoparticle dispersion on the melting of PCM in hemicylindrical cell. 12th IIR Conference on Phase-Change Materials and Slurries for Refrigeration and Air Conditioning (PCM 2018), Orford (Québec), Canada, 2018. https://doi.org/10.18462/iir.pcm.2018.0033.

[13] Radomska E., Mika L., Sztekler K., Lis L., The impact of heat exchangers' constructions on the melting and solidification time of phase change materials. Energies, 2020, 13(18): 4840. https://doi.org/10.3390/en13184840.

[14] Zayed M.E., Zhao J., Li W., Elsheikh A.H., Elbanna A.M., Jing L., Geweda A.E., Recent progress in phase change materials storage containers: Geometries, design considerations and heat transfer improvement methods. Journal of Energy Storage, 2022, 30: 101341. https://doi.org/10.1016/j.est.2020.101341.

[15] Dhaidan N.S., Khodadadi J.M., Melting and convection of phase change materials in different shape containers: a review. Renewable and Sustainable Energy Reviews, 2015, 43: 449–477. https://doi.org/10.1016/j.rser.2014.11.017.

[16] Li Z., Zhang Q., Wang Z., Li J., Experimental study on melting process in an industrial level molten salt tank. Journal of Thermal Science, 2020, 29: 457–463. https://doi.org/10.1007/s11630-019-1125-5.

[17] Dhaidan N.S., Melting phase change of n-eicosane inside triangular cavity of two orientations. Journal of Renewable and Sustainable Energy, 2017, 9(5): 054101. https://doi.org/10.1063/1.5007894.

[18] Thenmozhi R., Sharmeela C., Natarajan P., Velraj R., Transient thermal management comparison of a microprocessor using PCMs in various configurations. Journal of Thermal Science, 2011, 20: 516–520. https://doi.org/10.1007/s11630-011-0504-3.

[19] Zivkovic B., Fujii I., An analysis of isothermal phase change of phase change material within rectangular and cylindrical containers. Solar Energy, 2001, 70(1): 51–61. https://doi.org/10.1016/S0038-092X(00)00112-2.

[20] Jiji L.M., Gaye S., Analysis of solidification and melting of PCM with energy generation. Applied Thermal Engineering, 2006, 26: 568–575. https://doi:10.1016/j.applthermaleng.2005.07.008.

[21] Vynnycky M., Kimura S., An analytical and numerical study of coupled transient natural convection and solidification in a rectangular enclosure. International

Journal of Heat and Mass Transfer, 2007, 50: 5204–5214. https://doi:10.1016/j.ijheatmasstransfer.2007.06.036.

[22] Lazaro A., Dolado P., Marín J.M., Zalba B., PCM-air heat exchangers for free-cooling applications in buildings: Experimental results of two real-scale prototypes. Energy Conversion and Management, 2009, 50: 439–443. https://doi:10.1016/j.enconman.2008.11.002.

[23] Vitorino N., Abrantes J.C.C., Frade J.R., Numerical solutions for mixed controlled solidification of phase change materials. International Journal of Heat and Mass Transfer, 2010, 53: 5335–5342.

[24] Dolado P., Lazaro A., Marin J.M., Zalba B., Characterization of melting and solidification in a real scale PCM-air heat exchanger: Numerical model and experimental validation. Energy Conversion and Management, 2011, 52: 1890–1907. http://dx.doi.org/10.1016/j.enconman.2010.11.017.

[25] Teggar M., Mezaache E., Numerical investigation of a pcm heat exchanger for latent cool storage. Energy Procedia, 2013, 36: 1310–1319. https://doi.org/10.1016/j.egypro.2013.07.149.

[26] Iten M., Liu S., Shukla A., Experimental study on the thermal performance of air-PCM unit. Building and Environment, 2016, 105: 128–139. http://dx.doi.org/10.1016/j.buildenv.2016.05.035.

[27] Prieto M.M., Gonzalez B., Fluid flow and heat transfer in PCM panels arranged vertically and horizontally for application in heating systems. Renewable Energy, 2016, 97: 331–343. http://dx.doi.org/10.1016/j.renene.2016.05.089.

[28] Waqas A., Kumar S., Thermal performance of latent heat storage for free cooling of buildings in a dry and hot climate: An experimental study. Energy and Buildings, 2011, 43: 2621–2630. http://dx.doi.org/10.1016/j.enbuild.2011.06.015.

[29] Hu H., Jin X., Zhang X., Effect of supercooling on the solidification process of the phase change material. Energy Procedia, 2017, 105: 4321–4327. https://doi.org/10.1016/j.egypro.2017.03.905.

[30] Zhou G., Zhu M., Xiang Y., Effect of percussion vibration on solidification of supercooled salt hydrate PCM in thermal storage unit. Renewable Energy, 2018, 126: 537–544. https://doi.org/10.1016/j.renene.2018.03.077.

[31] Allouhia A., Ait Msaada A., Amineb M.B., et al., Optimization of melting and solidification processes of PCM: Application to integrated collector storage solar water heaters (ICSSWH). Solar Energy, 2018, 171: 562–570. https://doi.org/10.1016/j.solener.2018.06.096.

[32] Kumar N., Chavez R., Banerjee D., Experimental validation of thermal performance of a plate heat exchanger (PHX) with phase change materials (PCM) for thermal energy storage (TES). 2018 17th IEEE Intersociety Conference on Thermal and Thermomechanical Phenomena in Electronic Systems (ITherm), San Diego, CA, USA. https://doi.org/10.1109/ITHERM.2018.8419529.

[33] Zarajabad O.G., Ahmadi R., Numerical investigation of different PCM volume on cold thermal energy storage system. Journal of Energy Storage, 2018, 17: 515–524. https://doi.org/10.1016/j.est.2018.04.013.

[34] Ghosh D., Guha C., Ghose J., Numerical investigation of paraffin wax solidification in spherical and rectangular cavity. Heat and Mass Transfer, 2019, 55: 3547–3559. https://doi.org/10.1007/s00231-019-02680-4.

[35] Nada S.A., Alshaer W.G., Saleh R.M., Thermal characteristics and energy saving of charging/discharging processes of PCM in air free cooling with minimal temperature differences. Alexandria Engineering Journal, 2019, 58(4): 1175–1190. https://doi.org/10.1016/j.aej.2019.10.002.

[36] Santos T., Kolokotroni M., Hopper N., Yearley K., Experimental study on the performance of a new encapsulation panel for PCM's to be used in the PCM-air heat exchanger. Energy Procedia, 2019, 161: 352–359. http://dx.doi.org/10.1016/j.egypro.2019.02.105.

[37] Bhamare D.K., Rathod M.K., Banerjee J., Numerical model for evaluating thermal performance of residential building roof integrated with inclined phase change material (PCM) layer. Journal of Building Engineering, 2020, 28: 101018. https://doi.org/10.1016/j.jobe.2019.101018.

[38] Elsheniti M.B., Hemedah M.A., Sorour M.M., El-Maghlany W.M., Novel enhanced conduction model for predicting performance of a PV panel cooled by PCM. Energy Conversion and Management, 2020, 205: 112456. https://doi.org/10.1016/j.enconman.2019.112456.

[39] Gürel B., Thermal performance evaluation for solidification process of latent heat thermal energy storage in a corrugated plate heat exchanger. Applied Thermal Engineering, 2020, 174: 115312. https://doi.org/10.1016/j.applthermaleng.2020.115312

[40] Patel J.R., Joshi V., Rathod M.K., Thermal performance investigations of the melting and solidification in differently shaped macro-capsules saturated with phase change material. Journal of Energy Storage, 2020, 31: 101635. https://doi.org/10.1016/j.est.2020.101635.

[41] Saitoh T., On the optimum design for latent heat thermal energy storage reservoir. Refrigeration, 1983, 58: 737–749.

[42] Barba A., Spiga M., Discharge mode for encapsulated PCMs in storage tanks. Solar Energy, 2003, 7: 141–148. https://doi.org/10.1016/S0038-092X(03)00117-8.

[43] Chan C.W., Tan F.L., Solidification inside a sphere—an experimental study. International Communications in

Heat and Mass Transfer, 2006, 33: 335–341. https://doi:10.1016/j.icheatmasstransfer.2005.10.010.

[44] Ismail K.A.R., Moraes R.I.R., A numerical and experimental investigation of different containers and PCM options for cold storage modular units for domestic applications. International Journal of Heat and Mass Transfer, 2009, 52: 4195–4202. https://doi:10.1016/j.ijheatmasstransfer.2009.04.031.

[45] Veerappan M., Kalaiselvam S., Iniyan S., Goic R., Phase change characteristic study of spherical PCMs in solar energy storage. Solar Energy, 2009, 83: 1245–1252. https://doi:10.1016/j.solener.2009.02.006.

[46] Wu S., Fang G., Liu X., Thermal performance simulations of a packed bed cool thermal energy storage system using n-tetradecane as phase change material. International Journal of Thermal Sciences, 2010, 49: 1752–1762. https://doi.org/10.1016/j.ijthermalsci.2010.03.014.

[47] Wu S., Fang G., Dynamic performances of solar heat storage system with packed bed using myristic acid as phase change material. Energy and Buildings, 2011, 43: 1091–1096. https://doi.org/10.1016/j.enbuild.2010.08.029.

[48] ElGhnam R.I., Abdelaziz R.A., Sakr M.H., Abdelrhman H.E., An experimental study of freezing and melting of water inside spherical capsules used in thermal energy storage systems. Ain Shams Engineering Journal, 2012, 3: 33–48. http://dx.doi.org/10.1016/j.asej.2011.10.004.

[49] Archibold A., Rahman M.M., Gonzalez-Aguilar J., Goswami D.Y., Stefanakos E.K., Romero M., Phase change and heat transfer numerical analysis during solidification on an encapsulated phase change material. Energy Procedia, 2014, 57: 653–661. https://doi.org/10.1016/j.egypro.2014.10.220.

[50] Elmozughi A.F., Solomon L., Oztekin A., Neti S., Encapsulated phase change material for high temperature thermal energy storage—Heat transfer analysis. International Journal of Heat and Mass Transfer, 2014, 78: 1135–1144. http://dx.doi.org/10.1016/j.ijheatmasstransfer.2014.07.087.

[51] Reddy R.M., Nallusamy N., Reddy K.H., The effect of PCM capsule material on the thermal energy storage system performance. International Scholarly Research Notices, 2014, Article ID: 529280. https://doi.org/10.1155/2014/529280.

[52] Chandrasekaran P., Cheralathan M., Velraj R., Effect of fill volume on solidification characteristics of DI (deionized) water in a spherical capsule-An experimental study. Energy, 2015, 90(1): 508–515. http://dx.doi.org/10.1016/j.energy.2015.07.086.

[53] Chandrasekaran P., Cheralathan M., Velraj R., Influence of the size of spherical capsule on solidification characteristics of DI (deionized water) water for a cool thermal energy storage system—An experimental study. Energy, 2015, 90: 807–813. http://dx.doi.org/10.1016/j.energy.2015.07.113.

[54] Asker M., Ganjehsarabi H., Coban M.T., Numerical investigation of inward solidification inside spherical capsule by using temperature transforming method. Ain Shams Engineering Journal, 2016, 9(4): 537–547. https://doi.org/10.1016/j.asej.2016.02.009.

[55] Ismail K.A.R., Moura L.F., Lago T., Lino F.A.M., Nobrega C., Experimental study of fusion and solidification of phase change material (PCM) in spherical geometry. 12th International Conference on Heat Transfer, Fluid Mechanics and Thermodynamics, 2016, Volume 1, Spain.

[56] Liu M.J., Fan L.W., Zhu Z.Q., Feng B., Zhang H.C., Zeng Y., A volume-shrinkage-based method for quantifying the inward solidification heat transfer of a phase change material filled in spherical capsules. Applied Thermal Engineering, 2016, 108: 1200–1205. http://dx.doi.org/10.1016/j.applthermaleng.2016.08.027.

[57] Pop O., Tutunaru L.F., Balan M., Numerical model for solidification and melting of PCM encapsulated in spherical shells. Energy Procedia, 2017, 112: 336–343. https://doi.org/10.1016/j.egypro.2017.03.1060.

[58] Ehms J., Oliveski R., Rocha L., Biserni C., Theoretical and numerical analysis on phase change materials (PCM): A case study of the solidification process of erythritol in spheres. International Journal of Heat and Mass Transfer, 2018, 119: 523–532. https://doi.org/10.1016/j.ijheatmasstransfer.2017.11.124.

[59] Nazififard M., Badri M.S., Najafzadeh S., Jowkar H., Visualization of phase change material solidification process in spherical geometry. The 26th Annual International Conference of Iranian Society of Mechanical Engineers-ISME2018, 24–26 April, 2018, School of Mechanical Engineering, Semnan University, Semnan, Iran.

[60] Loem S., Deethayat T., Asanakham A., Kiatsiriroat T., Thermal characteristics on melting/solidification of low temperature PCM balls packed bed with air charging/discharging. Case Studies in Thermal Engineering, 2019, 14: 100431. https://doi.org/10.1016/j.csite.2019.100431

[61] Mawire A., Lentswe K., Okello D., Lugolole R., Nyeinga K., Shobo A., Dynamic thermal performance of four encapsulated PCM spheres for domestic medium temperature applications. Energy Procedia, 2019, 158: 4375–4382. https://doi.org/10.1016/j.egypro.2019.01.781

[62] Vikram M.P., Kumaresan V., Christopher S., Velraj R., Experimental studies on solidification and subcooling characteristics of water-based phase change material (PCM) in a spherical encapsulation for cool thermal

energy storage applications. International Journal of Refrigeration, 2019, 100: 454–462. https://doi.org/10.1016/j.ijrefrig.2018.11.025.

[63] Gao J.Y., Zhang X.D., Fu J.H., Yang X.H., Liu J., Numerical investigation on integrated thermal management via liquid convection and phase change in packed bed of spherical low melting point metal macrocapsules. International Journal of Heat and Mass Transfer, 2020, 150: 119366. https://doi.org/10.1016/j.ijheatmasstransfer.2020.119366.

[64] Lago T.G.S., Ismail K.A.R., Lino F.A.M., Arabkoohsar A., Experimental correlations for the solidification and fusion times of PCM encapsulated in spherical shells. Experimental Heat Transfer, 2020, 33(5): 440–454. https://doi.org/10.1080/08916152.2019.1656301.

[65] Gao X., Zhang W., Fang Z., Hou X., Zhang X., Analysis of melting and solidification processes in the phase-change device of an energy storage interconnected heat pump system. AIP Advances, 2020, 10: 055021. https://doi.org/10.1063/5.0006280.

[66] Lipnicki Z., Małolepszy T., Gortych M., Grabas P., Simple analytical and experimental method of solidification PCM material inside a spherical capsule. International Communications in Heat and Mass Transfer, 2022, 135: 106083. https://doi.org/10.1016/j.icheatmasstransfer.2022.106083.

[67] Sarbu I., Sebarchievici C., A comprehensive review of thermal energy storage. Sustainability, 2018, 10(1): 191. https://doi.org/10.3390/su10010191.

[68] Bilir L., Ilken Z., Total solidification time of a liquid phase change material enclosed in cylindrical/spherical containers. Applied Thermal Engineering, 2005, 25: 1488–1502. https://doi:10.1016/j.applthermaleng.2004.10.005.

[69] Kalaiselvam S., Veerappan M., Aaronb A.A., Iniyan S., Experimental and analytical investigation of solidification and melting characteristics of PCMs inside cylindrical encapsulation. International Journal of Thermal Sciences, 2008, 47: 858–874. https://doi:10.1016/j.ijthermalsci.2007.07.003.

[70] Lu J.F., Ding J., Yang J.P., Solidification and melting behaviors and characteristics of molten salt in cold filling pipe. International Journal of Heat and Mass Transfer, 2010, 53: 1628–1635. http://dx.doi.org/10.1016/j.ijheatmasstransfer.2010.01.033.

[71] Rajeev K., Das S., A numerical study for inward solidification of a liquid contained in cylindrical and spherical vessel. Thermal Science, 2010, 14(2): 365–372. https://doi.org/10.2298/TSCI1002365R.

[72] Sridharan P., Aspect ratio effect on melting and solidification during thermal energy storage. University of South Florida, 2013. https://scholarcommons.usf.edu/etd/4777/.

[73] Motahar S., Khodabandeh R., Experimental study on the melting and solidification of a phase change material enhanced by heat pipe. International Communications in Heat and Mass Transfer, 2016, 73: 1–6. http://dx.doi.org/10.1016/j.icheatmasstransfer.2016.02.012.

[74] Alexiadis A., Ghraybehb S., Qiaoc G., Natural convection and solidification of phase-change materials in circular pipes: A SPH approach. Computational Materials Science, 2018, 150: 475–483. https://doi.org/10.1016/j.commatsci.2018.04.037.

[75] Stamatiou A., Maranda S., Eckl F., Schuetz P., Fischer L., Worlitschek J., Quasi-stationary modelling of solidification in a latent heat storage comprising a plain tube heat exchanger. Journal of Energy Storage, 2018, 20: 551–559. https://doi.org/10.1016/j.est.2018.10.019.

[76] Han X., Kang Z., Tian X., Wang L., Experimental observations on the interface front of phase change material inside cylindrical cavity. Energy Storage, 2019, 1(1): e36. https://doi.org/10.1002/est2.36.

[77] Izgi B., Arslan M., Numerical analysis of solidification of PCM in a closed vertical cylinder for thermal energy storage applications. Heat and Mass Transfer, 2020, 56: 2909–2922. https://doi.org/10.1007/s00231-020-02911-z.

[78] Olfian H., Ajarostaghi S.S.M., Farhadi M., Ramiar A., Melting and solidification processes of phase change material in evacuated tube solar collector with U-shaped spirally corrugated tube. Applied Thermal Engineering, 2021, 182: 116149. https://doi.org/10.1016/j.applthermaleng.2020.116149.

[79] Lacroix M., Study of heat transfer behaviour of a latent heat thermal energy storage unit with a finned tube. International Journal of Heat Mass Transfer, 1993, 36(8): 2083–2092. https://doi.org/10.1016/S0017-9310(05)80139-5.

[80] Agyenim F., Hewitt N., Eames P., Smyth M., A review of materials, heat transfer and phase change problem formulation for latent heat thermal energy storage systems (LHTESS). Renewable and Sustainable Energy Reviews, 2010, 14: 615–628. https://doi.org/10.1016/j.rser.2009.10.015.

[81] Trp A., An experimental and numerical investigation of heat transfer during technical grade paraffin melting and solidification in a shell-and-tube latent thermal energy storage unit. Solar Energy, 2005, 79: 648–660. https://doi:10.1016/j.solener.2005.03.006.

[82] Long J.Y., Numerical and experimental investigation for heat transfer in triplex concentric tube with phase change material for thermal energy storage. Solar Energy, 2008, 82: 977–985. https://doi:10.1016/j.solener.2008.05.006.

[83] Ezan M.A., Ozdogan M., Erek A., Experimental study on

charging and discharging periods of water in a latent heat storage unit. International Journal of Thermal Sciences, 2011, 50: 2205–2219. http://dx.doi.org/10.1016/j.ijthermalsci.2011.06.010.

[84] Lipnicki Z., Weigand B., An experimental and theoretical study of solidification in a free-convection flow inside a vertical annular enclosure. International Journal of Heat and Mass Transfer, 2012, 55: 655–664. http://dx.doi.org/10.1016/j.ijheatmasstransfer.2011.10.044.

[85] Longeon M., Soupart A., Fourmigué J.F., Bruch A., Marty P., Experimental and numerical study of annular PCM storage in the presence of natural convection. Applied Energy, 2013, 112: 175–184. http://dx.doi.org/10.1016/j.apenergy.2013.06.007.

[86] Avci M., Yazici M.Y., Experimental study of thermal energy storage characteristics of a paraffin in a horizontal tube-in-shell storage unit. Energy Conversion and Management, 2013, 73: 271–277. http://dx.doi.org/10.1016/j.enconman.2013.04.030.

[87] Solomon G.R., Karthikeyan S., Velraj R., Sub cooling of PCM due to various effects during solidification in a vertical concentric tube thermal storage unit. Applied Thermal Engineering, 2013, 52: 505–511. http://dx.doi.org/10.1016/j.applthermaleng.2012.12.030.

[88] Jesumathy S.P., Udayakumar M., Suresh S., Jegadheeswaran S., An experimental study on heat transfer characteristics of paraffin wax in horizontal double pipe heat latent heat storage unit. Journal of the Taiwan Institute of Chemical Engineers, 2014, 45(4): 1298–1306. https://doi.org/10.1016/j.jtice.2014.03.007.

[89] Hosseini M.J., Rahimi M., Bahrampoury R., Experimental and computational evolution of a shell and tube heat exchanger as a PCM thermal storage system. International Communications in Heat and Mass Transfer, 2014, 50: 128–136. https://doi.org/10.1016/j.icheatmasstransfer.2013.11.008.

[90] Ismail K.R., Lino F.M., Da Silva R.R., De Jesus A.B., Paixão L.C., Experimentally validated two dimensional numerical model for the solidification of PCM along a horizontal long tube. International Journal of Thermal Sciences, 2014, 75: 184–193. http://dx.doi.org/10.1016/j.ijthermalsci.2013.08.008

[91] Kibria M.A., Anisur M.R., Mahfuz M.H., Saidur R., Metselaar I.H.S.C., Numerical and experimental investigation of heat transfer in a shell and tube thermal energy storage system. International Communications in Heat and Mass Transfer, 2014, 53: 71–78. https://doi.org/10.1016/j.icheatmasstransfer.2014.02.023.

[92] Yazici M.Y., Avci M., Aydin O., Akgun M., On the effect of eccentricity of a horizontal tube-in-shell storage unit on solidification of a PCM. Applied Thermal Engineering, 2014, 64: 1–9. http://dx.doi.org/10.1016/j.applthermaleng.2013.12.005.

[93] Bechiri M., Mansouri K., Analytical solution of heat transfer in a shell-and-tube latent thermal energy storage system. Renewable Energy, 2015, 74: 825–838. http://dx.doi.org/10.1016/j.renene.2014.09.010.

[94] Agarwal A., Sarviya R.M., An experimental investigation of shell and tube latent heat storage for solar dryer using paraffin wax as heat storage material. Engineering Science and Technology, an International Journal, 2016, 19(1): 619–631. https://doi.org/10.1016/j.jestch.2015.09.014.

[95] Seddegh S., Wang X., Henderson A.D., A comparative study of thermal behavior of a horizontal and vertical shell-and-tube energy storage using phase change materials. Applied Thermal Engineering, 2016, 93: 348–358. https://doi.org/10.1016/j.applthermaleng.2015.09.107.

[96] Wang Y., Wang L., Xie N., Lin X., Chen H., Experimental study on the melting and solidification behavior of erythritol in a vertical shell-and-tube latent heat thermal storage unit. International Journal of Heat and Mass Transfer, 2016, 99: 770–781. http://dx.doi.org/10.1016/j.ijheatmasstransfer.2016.03.125.

[97] Ma Z., Bao H., Roskilly A.P., Study on solidification process of sodium acetate trihydrate for seasonal solar thermal energy storage. Solar Energy Materials and Solar Cells, 2017, 172: 99–107. http://dx.doi.org/10.1016/j.solmat.2017.07.024.

[98] Riahi S., Saman W.Y., Bruno F., Belusko M., Tay N.H.S., Impact of periodic flow reversal of heat transfer fluid on the melting and solidification processes in a latent heat shell and tube storage system. Applied Energy, 2017, 191: 276–286. http://dx.doi.org/10.1016/j.apenergy.2017.01.091.

[99] Riahi S., Saman W.Y., Bruno F., Belusko M., Tay N.H.S., Comparative study of melting and solidification processes in different configurations of shell and tube high temperature latent heat storage system. Solar Energy, 2017, 150: 363–374. http://dx.doi.org/10.1016/j.solener.2017.04.061.

[100] Tao Y.B., Liu Y.K., He Y.L., Effects of PCM arrangement and natural convection on charging and discharging performance of shell-and-tube LHS unit. International Journal of Heat and Mass Transfer, 2017, 115: 99–107. http://dx.doi.org/10.1016/j.ijheatmasstransfer.2017.07.098.

[101] Elmeriah A., Nehari D., Aichouni M., Thermo-convective study of a shell and tube thermal energy storage unit. Periodica Polytechnica Mechanical Engineering, 2018, 62(2): 101–109. https://doi.org/10.3311/PPme.10873.

[102] Tehrani S.S.M., Diarce G., Taylor R.A., The error of neglecting natural convection in high temperature vertical shell-and-tube latent heat thermal energy storage systems.

Solar Energy, 2018, 174: 489–501.
https://doi.org/10.1016/j.solener.2018.09.048.

[103] Mehta D.S., Solanki K., Rathod M.K., Banerjee J, Thermal performance of shell and tube latent heat storage unit: Comparative assessment of horizontal and vertical orientation. Journal of Energy Storage, 2019, 23: 344–362.
https://doi.org/10.1016/j.est.2019.03.007.

[104] Sodhi G.S., Jaiswal A.K., Vigneshwaran K., Muthukumar P., Investigation of charging and discharging characteristics of a horizontal conical shell and tube latent thermal energy storage device. Energy Conversion and Management, 2019, 188: 381–397.
https://doi.org/10.1016/j.enconman.2019.03.022.

[105] Andrzejczyk R., Kozak P., Muszynski T., Experimental investigations on the influence of coil arrangement on melting/solidification processes. Energies, 2020, 13: 6334.
https://doi:10.3390/en13236334.